18

Deckelman, J. A., S. Chi, A. K. Hartwig, K. R. Reuber, and J. Fruehn, 2021, The role of megaregional seismic data in Santos Basin pre-salt exploration and development, *in* Marcio R. Mello, Pinar O. Yilmaz, and Barry J. Katz, eds., The supergiant Lower Cretaceous pre-salt petroleum systems of the Santos Basin, Brazil: AAPG Memoir 124, p. 487–516.

The Role of Megaregional Seismic Data in Santos Basin Pre-Salt Exploration and Development

J. A. Deckelman, S. Chi, A. K. Hartwig, K. R. Reuber, and J. Fruehn

ION Geophysical, 2105 CityWest Blvd., Suite 900, Houston, Texas, 77042 USA (e-mails: James.Deckelman@iongeo.com; Shihong.Chi@iongeo.com; Andrew.Hartwig@iongeo.com; Kyle.Reuber@iongeo.com; Juergen.Fruehn@iongeo.com)

ABSTRACT

More than 45 billion barrels of recoverable oil have been discovered in the Santos and Campos Basin pre-salt play to date. The prolific nature of this play relates to a supercharged Barremian-to-Aptian synrift petroleum system; a regionally extensive Aptian evaporite top seal; an extraordinary combination of high-storage capacity, high deliverability, undersaturated and overpressured lacustrine carbonate reservoirs; excellent crude oil quality (in areas that are CO_2-poor); and large closure areas with access to multiple thermally mature, oil-prone source kitchens.

A calibrated megaregional 3-D seismic data volume is a critical factor in the development and understanding of the Santos Basin pre-salt play. The data volume comprises more than 99,000 km^2 of mixed-vintage, mixed-azimuth 3-D seismic data, which were consistently prestack depth migrated (PSDM), reimaged using a calibrated anisotropic velocity model, and consistently datumed, amplitude balanced, and phase matched.

The data have application to both pre-salt exploration and pre-salt field development. At basin scale, the data are used to define a 210,000 km^2 pre-salt play fairway and to understand controls on pre-salt hydrocarbon accumulation. At field and reservoir scales, inverted elastic seismic data attributes and data analytics are used to determine and predict reservoir and fluid properties, thereby enabling effective field appraisal and development.

INTRODUCTION

Location and Structural Setting

The Santos Basin is located in southern Brazil, south of the city of Rio de Janeiro. It extends from the Serra do Mar coastal range southeastward into the Atlantic Ocean, into water depths in excess of 3500 m, and encompasses an area greater than 350,000 km^2.

The Santos Basin is a South Atlantic extensional continental margin bounded by the Cabo Frio High to the north and the Florianopolis High and Florianopolis Fracture Zone to the south (Figure 1). Between these features lies the Santos Basin Outer High,

DOI: 10.1306/13722330MSB.17.1853

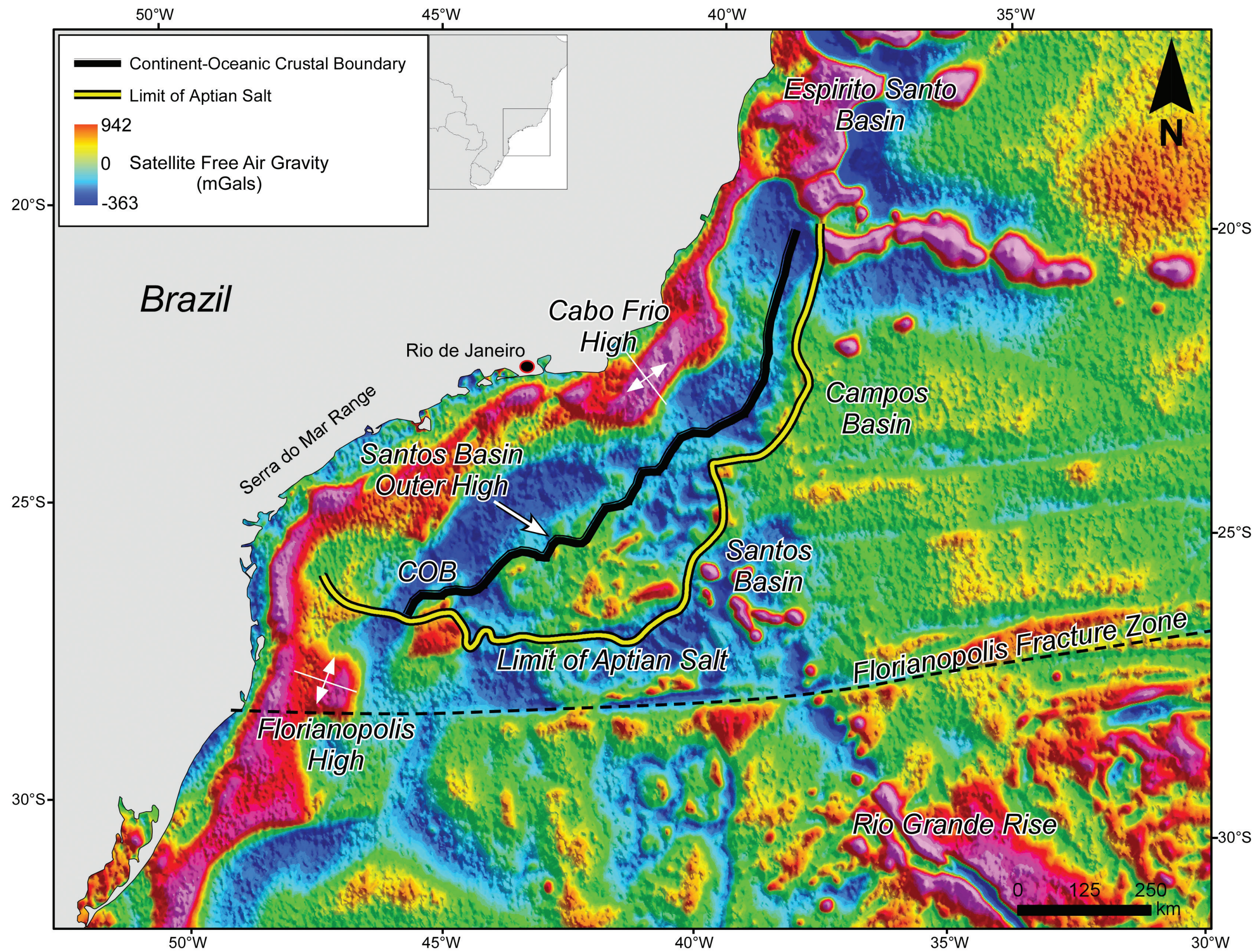

Figure 1. Sandwell et al. (2014) satellite free-air gravity map showing Santos Basin major structural elements, the seaward limit of Aptian salt, and the continental-oceanic crustal boundary (COB).

a regional top-basement and base salt (top post-rift sag) structural high (Figure 2). The Santos Basin Outer High contains multiple large culminations that serve as important regional hydrocarbon migration foci. The Tupi (Lula) Field, one of the largest petroleum accumulations in Brazil, forms one such culmination. The paleotopographic relief of the Outer High resulted in a clastic-starved fresh-water lacustrine environment, ideal for the development of a broad carbonate platform in lower Aptian time (Gomes et al., 2009).

The Santos Basin forms part of the western South Atlantic margin and is conjugate to the Namibe Basin of southern Angola (Figure 3). The Namibe Basin lies north of the Walvis Ridge, a South Atlantic volcanic hotspot track that marks the southern limit of the Aptian salt on the African margin. On the conjugate Brazilian margin, the Florianopolis High demarcates the southern limit of Aptian salt.

The Santos and Namibe basins form an asymmetric conjugate margin pair (Hurst et al., 2020; Figures 3, 6). The formation of this asymmetric pair may be related to the development of a Santos Basin ridge jump and consequent sea floor spreading east of the Santos Basin Outer High, resulting in a relatively wider Santos margin (Hurst et al., 2020).

Only two petroleum exploration wells have been drilled in the offshore Namibe Basin, there is only one Ocean Drilling Program (ODP) well, and there are no offshore Namibe Basin pre-salt penetrations. As such, the authors' understanding of Namibe Basin stratigraphy is based on onshore data. Although both margins are thought to share generally common Albian

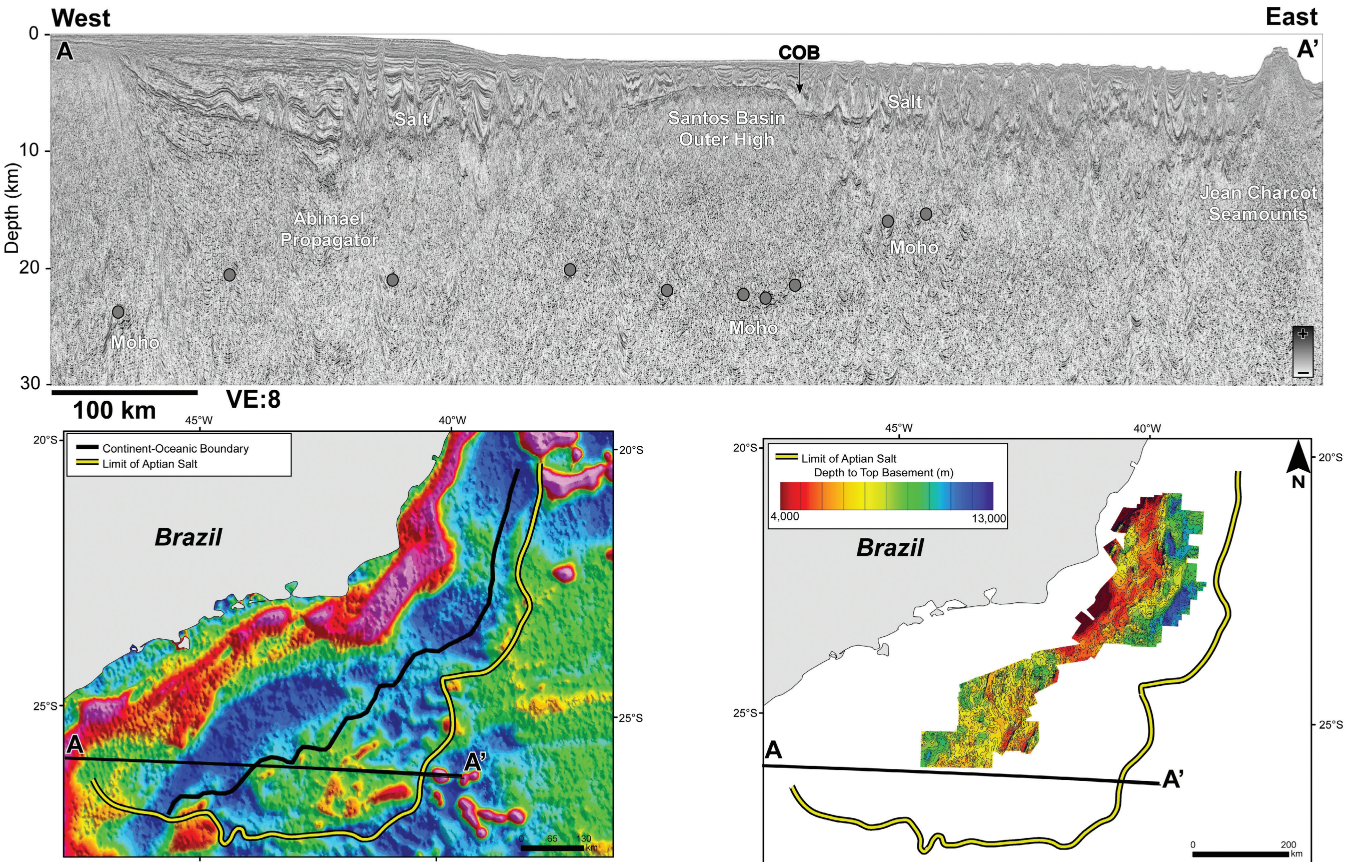

Figure 2. 2-D seismic transect across the Santos Basin Outer High showing Santos Basin major structural elements.

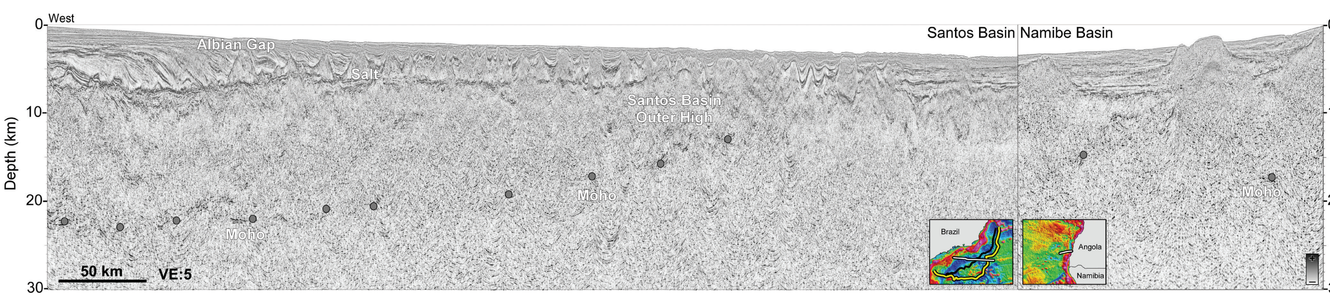

Figure 3. Conjugate PSDM seismic profiles across the South Atlantic at 113 ma (late Aptian). Santos Basin, Brazil to the west; Namibe Basin, Angola to the east. In the Santos Basin (left), note the well-expressed MOHO at ~22 km depth; faulted, rotated half-graben with syn-rift fill; downslope-rafted Albian carbonates, basinward-prograding post-Albian sediments filling "Albian Gap" accommodation space; thick, mobile salt; and the Santos Basin Outer High.

and older stratigraphy, the Namibe Basin Cenomanian and younger passive margin sequence contain greater amounts of volcanics and coarse-grained clastics.

The Santos Basin originated in late Valangian to early Aptian time during two phases of crustal extension. Both are associated with continental breakup and opening of the South Atlantic. This extension created accommodation space for more than 2 km of synrift sediment and resulted in extensive graben and half-graben development. Many half-graben display synrift stratal rotation and thickening into bounding high-angle normal faults. Thermal subsidence led to the development of a post-rift sag basin in the ensuing approximately 13 m.y., which was followed by greater than 112 m.y. of westward relative passive margin drift.

Stratigraphy

The Santos Basin contains greater than 9 km of Pleistocene–to–Lower Cretaceous volcanic and sedimentary fill (Figure 4). It overlies Precambrian crystalline and metamorphic continental crust inboard and Neocomian oceanic crust outboard. The location of the continent-ocean boundary (COB), shown on Figures 1 and 2, is constrained by 2-D and 3-D seismic data.

The stratigraphic section comprises a Valangian–to–lower Aptian synrift sequence, a middle and upper Aptian post-rift sag sequence, and an Albian-to-Pleistocene post-rift drift sequence (Figure 5; Moreira et al., 2007).

The synrift sequence is divided into lower and upper parts, each representing a separate phase of crustal extension and rifting. Lower synrift sediments comprise Valangian/Hauterivian volcanics and conglomerates of the Camboriu Formation. They are time equivalent to the Cabiúnas Formation in the Campos Basin and the Etendeka Formation of the conjugate Namibe Basin, Angola (Figure 6). Upper synrift sediments comprise Barremian to lower Aptian lacustrine sediments of the Picarras and Itapema formations. Widespread rifting enabled the development of an extensive area of interconnected lacustrine basins, periodically isolated and filled with thick successions of dominant lacustrine (and locally alluvial and fluvial) sediments (Thompson et al., 2015).

On the Santos Basin shelf, the Barra Velha Formation post-rift sag sequence comprises alluvial and lacustrine conglomerates, sandstone (the Atafona sandstone),

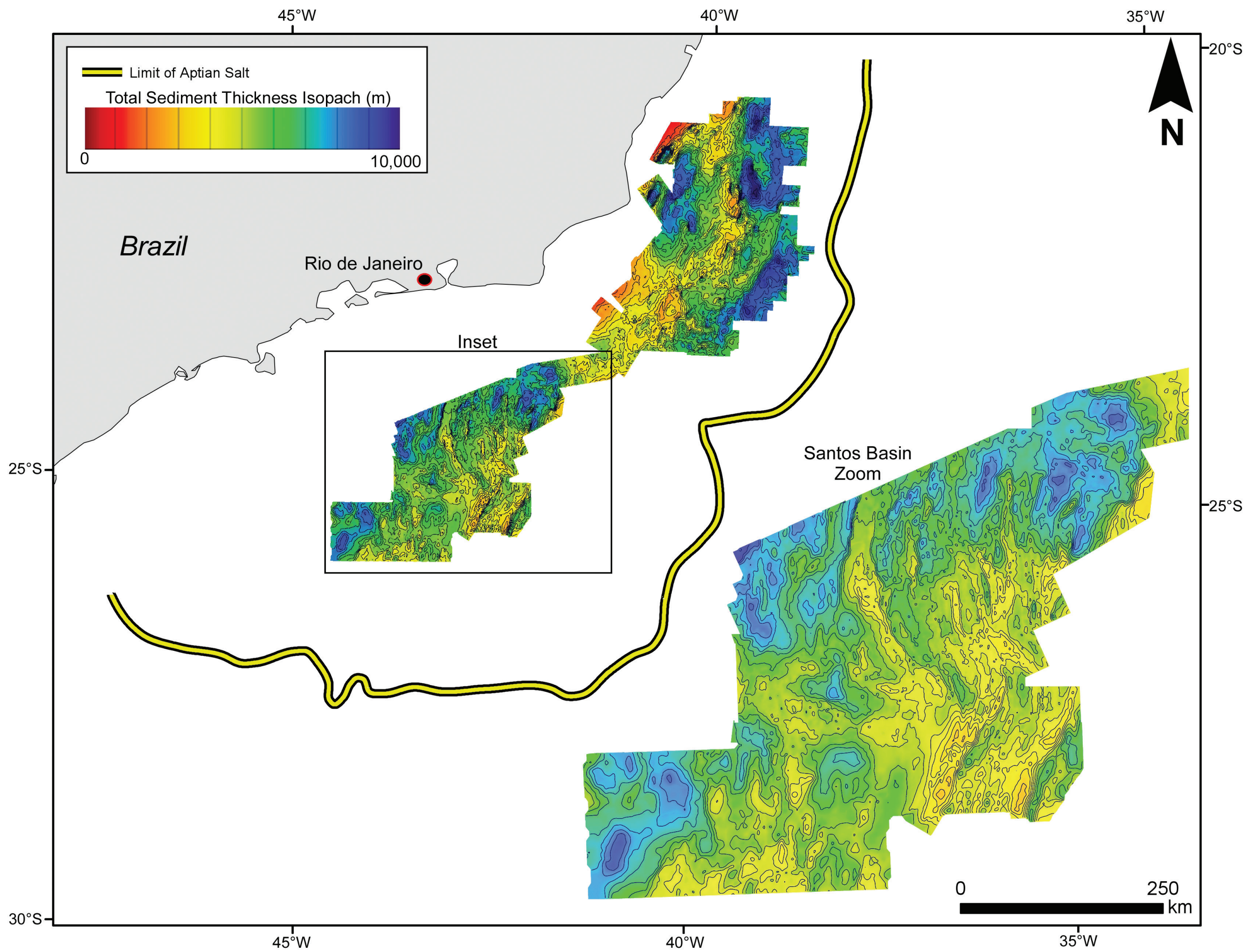

Figure 4. Santos and Campos Basins total sediment thickness map (seafloor to base syn-rift [top Basement]).

and lacustrine coquinas. These grade seaward into the lacustrine coquinas and overlying microbialites, hundreds of meters thick on the Santos Basin Outer High. The sag sequence is disconformable and unconformably overlies the synrift sequence (Figure 5).

The sag sequence is overlain by a locally thick (>2 km) accumulation of Aptian halite and anhydrite deposited in an arid hypersaline environment. Aptian sediments grade upward into Albian carbonates and clastics. In the inboard parts of the Santos Basin, Albian carbonates are rafted downdip on the base Aptian salt detachment.

Albian strata are overlain by a Cenomanian-to-Pleistocene passive-margin continental-drift sequence comprising fine and coarse-grained marine clastics and minor carbonates.

EVOLUTION OF THE PRE-SALT PLAY

The first Santos/Campos basin well to encounter petroleum in the pre-salt sequence was the Petrobras 1-RJS-013 well. It was drilled in 1975 on the Campos Basin shelf at what is now Badejo Field (IHS Markit, 2020). It was drilled in 90 m of water, inboard of the highly prolific Oligo-Miocene turbidite play that hosts giant post-salt fields such as Albacora, Marlim, Marlim Sul, Marlim Leste, Barracuda, and Caratinga. The well targeted a highly faulted structural high at multiple pre-salt levels. It commenced pre-salt production in 1981 and reached peak production of 9288 BOPD (3.39 MMBO/y) in 1986. It was the first field to produce from pre-salt (synrift) fractured basalts and the first to encounter oil in pre-salt coquinas (IHS Markit, 2020).

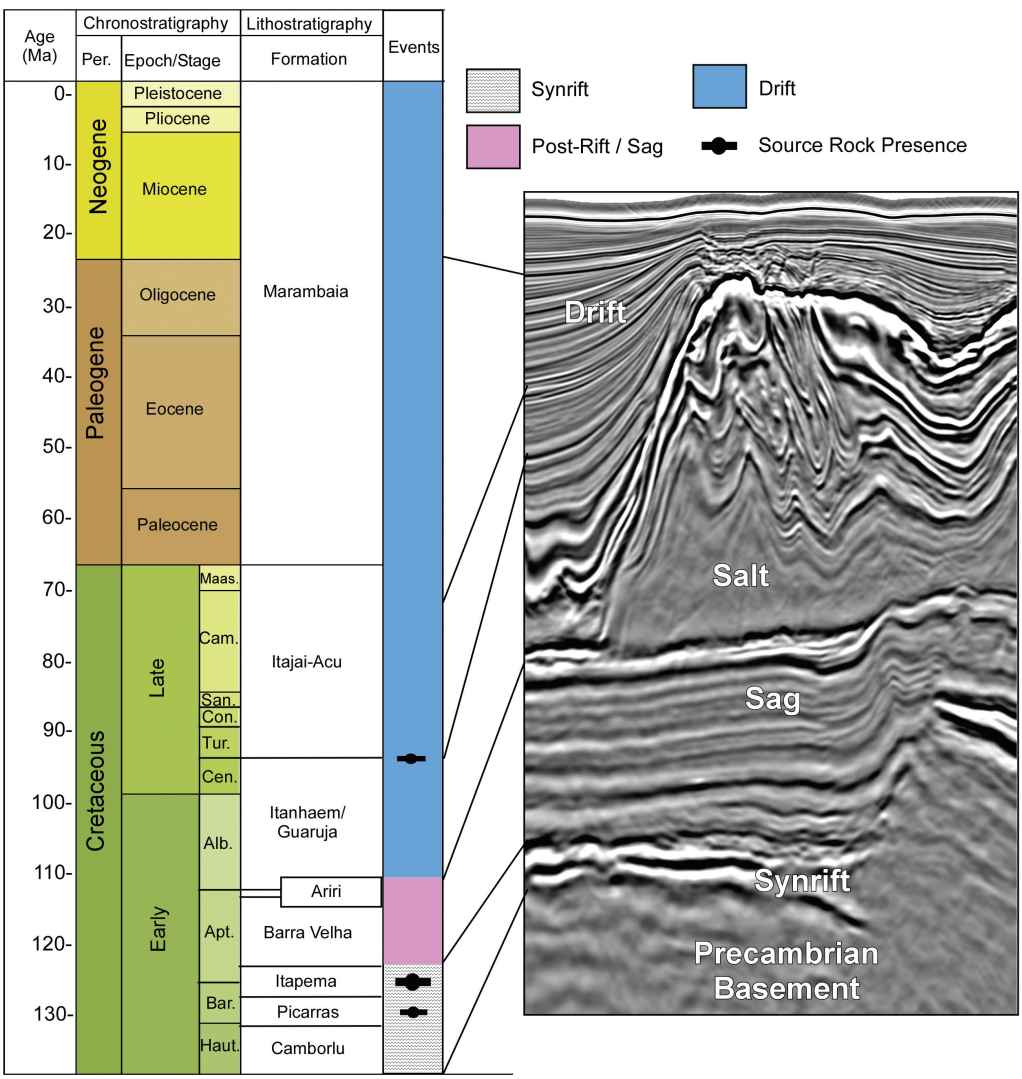

Figure 5. Stratigraphy of the Santos Basin, Brazil (modified from Moreira et al., 2007).

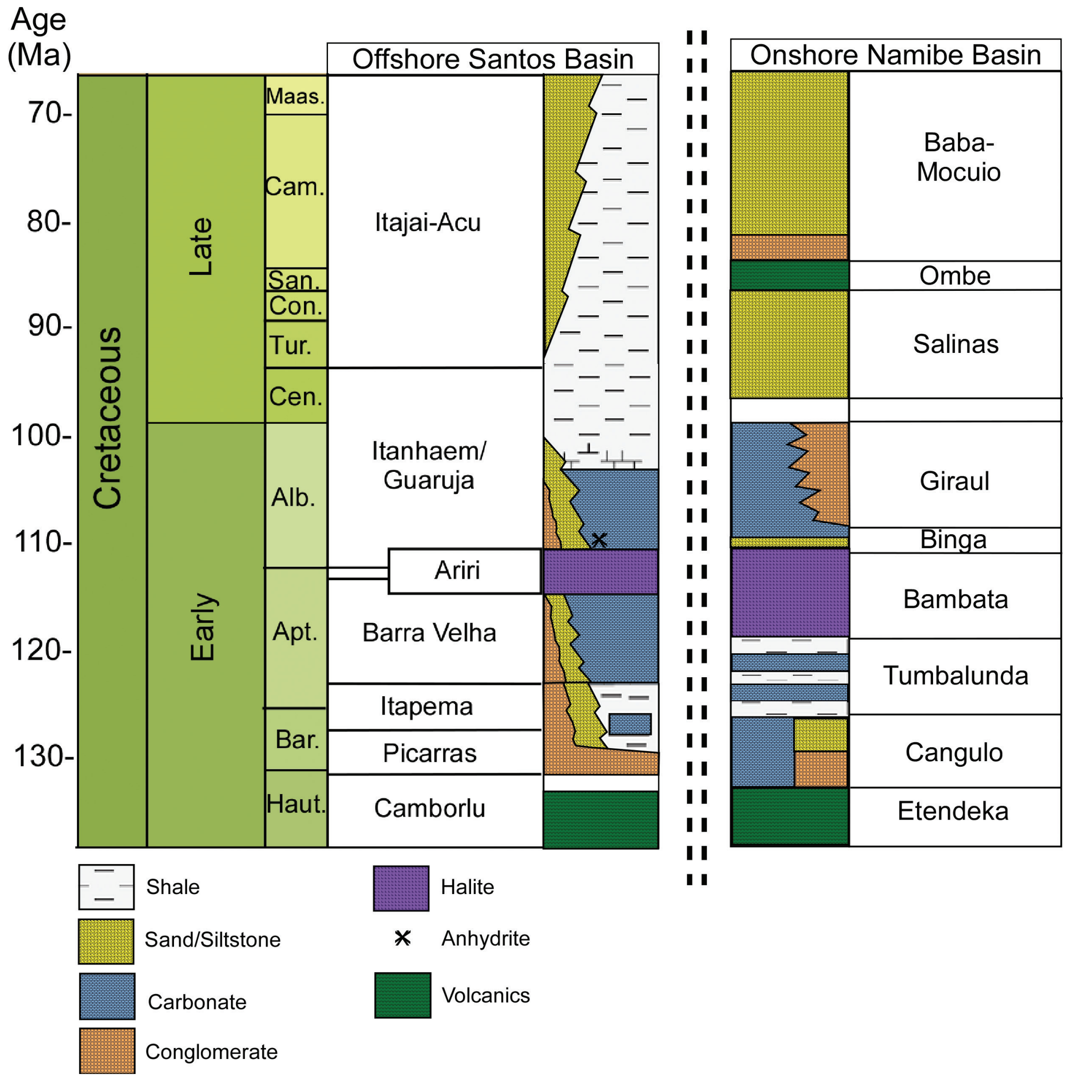

Figure 6. Generalized stratigraphic correlation of the Santos Basin, Brazil, with the conjugate Namibe Basin, Angola (modified from Schroder et al., 2016).

Although many pre-salt wells were drilled in the years that followed, and some wells or fields produced limited volumes of pre-salt hydrocarbons, it was not until 2008 when significant, sustained commercial pre-salt production was established at the Campos Basin's Jubarte Field (Figure 8).

In the Campos Basin where initial pre-salt drilling took place, several factors contributed to the lack of commercial success. These include the lack of a well-developed salt seal, the lack of effective structural and/or stratigraphic traps at pre-salt level, and the lack of charge to high-porosity pre-salt Atafona sandstones. Most important, however, coquina and other pre-salt carbonate lithologies were of poor reservoir quality (low permeability and 3%–12% porosity), unlike the much higher reservoir quality coquina reservoirs that occur in the deep-water Santos Basin. Additionally, pre-salt microbialite reservoirs were absent.

In the decades that followed, technical advances were made on many fronts. The importance of Santos Basin Outer High (Figure 2) became clear. It was recognized as an area of regional migration focus from kitchen areas to the north, west, and possibly east; an area that contains large pre-salt structural closures, a clastic-starved area favorable for pre-salt carbonate reservoir development; and an area containing a thick salt seal (Gomes et al., 2009).

Seismic data coverage was limited, however, and existing seismic technology failed to adequately resolve essential petroleum system elements beneath the thick (>2 km) salt seal. Subsequent advances in seismic imaging technology, principally pre-stack depth migration (PSDM) and improved velocity modeling, enabled pre-salt geology to be clearly imaged, ultimately unlocking the pre-salt play. Seismic technology currently employed in pre-salt exploration includes reverse time migration (RTM), greatly improved tomography, and full waveform inversion (FWI; Fruehn et al., 2019).

These advancements led to the discovery of the giant (5.5 billion barrels recoverable) Tupi Field (formerly “Lula” Field) in 2006 (IHS Markit, 2020). Since that time, more than 50 pre-salt discoveries have been made, rendering the Santos Basin one of the most important oil- and gas-producing provinces in the world. As of January 2020, 16.4 billion barrels of 2P (proved + probable) reserves were ascribed to the Santos Basin, and the production reached around 2.06 million barrels of oil per day (2.59 MMBOE/d) (Avila, 2017; ANP Bulletin, 2020). This accounted for 66% of Brazil’s total production. In total, more than 45 billion barrels of original recoverable oil resource are ascribed to the Santos and Campos basins pre-salt play (IHS Markit, 2020; Figure 7).

As of October 2020, 61 of 70 pre-salt exploration wells had encountered moveable hydrocarbons, resulting in an 87% geological success rate (Mello et al., 2020). The Santos and Campos basins pre-salt commercial success rates are approximately 51% (IHS Markit, 2020).

The prolific nature of the Santos Basin relates to a supercharged pre-salt petroleum system; an extraordinary combination of high-storage capacity, high deliverability, undersaturated and overpressured reservoirs; excellent crude oil quality (except where CO_2 rich); large closure areas; and oil columns locally in excess of 600 m in height.

The play extends from the Santos to the Campos and Espirito Santo basins over an area of approximately 210,000 km^2 (Figure 8). The presence of many undrilled traps within the pre-salt play fairway and creaming curve analysis suggest the pre-salt play has billions of barrels remaining undiscovered resource potential.

DATABASE AND METHODOLOGY

The database for this study comprises the following:

1. ION Geophysical’s 99,275 km^2 Picanha anisotropic PSDM 3-D seismic data volume, with Kirchhoff and RTM migration
2. ION Geophysical’s *BrasilSPAN* 10 km offset, 18 s record length (~40 km depth migrated) 2-D seismic data set
3. Towed gravity and magnetic data acquired with *BrasilSPAN* 2-D seismic data
4. One hundred seventy-four wells
5. Other relevant proprietary and public-domain technical data and industry information (Figure 9)

ION’s Picanha 3-D data volume comprises more than 99,000 km^2 of previously discrete, mixed-vintage, mixed-azimuth 3-D seismic data, consistently PSDM

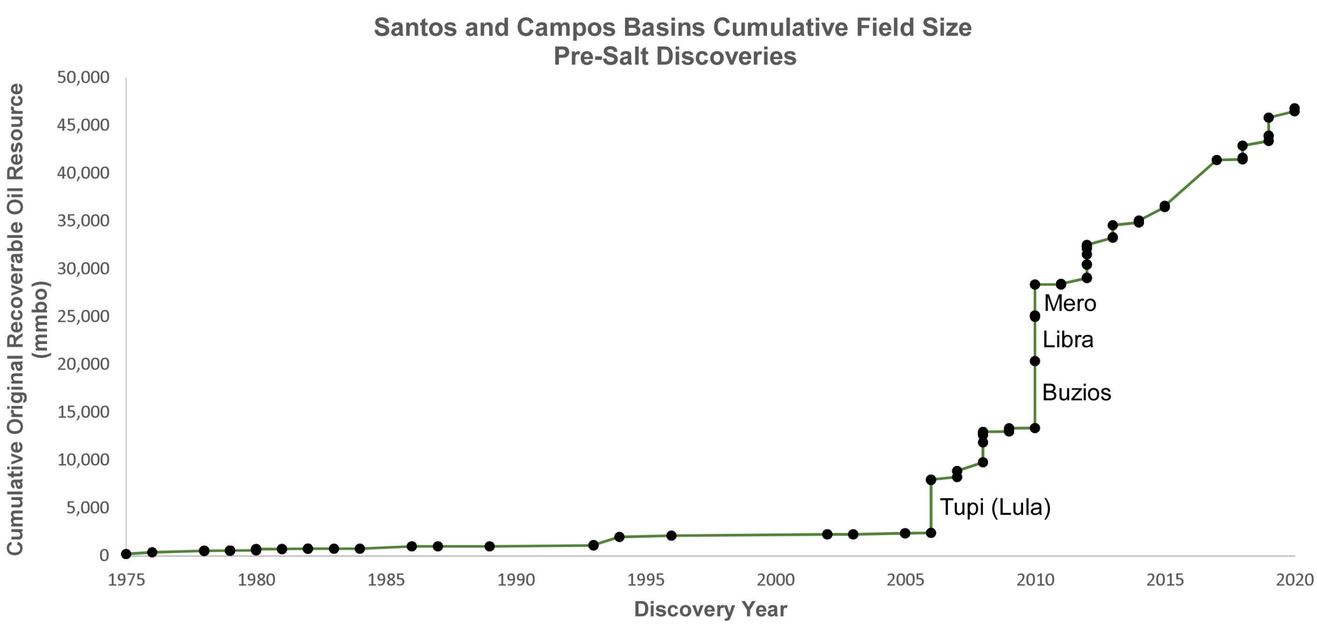

Figure 7. Santos and Campos Basins pre-salt creaming curve showing cumulative original recoverable oil resource volume (mmbo) by field (dots) and year (IHS Markit, 2020). Volumes are as estimated at the time of discovery.

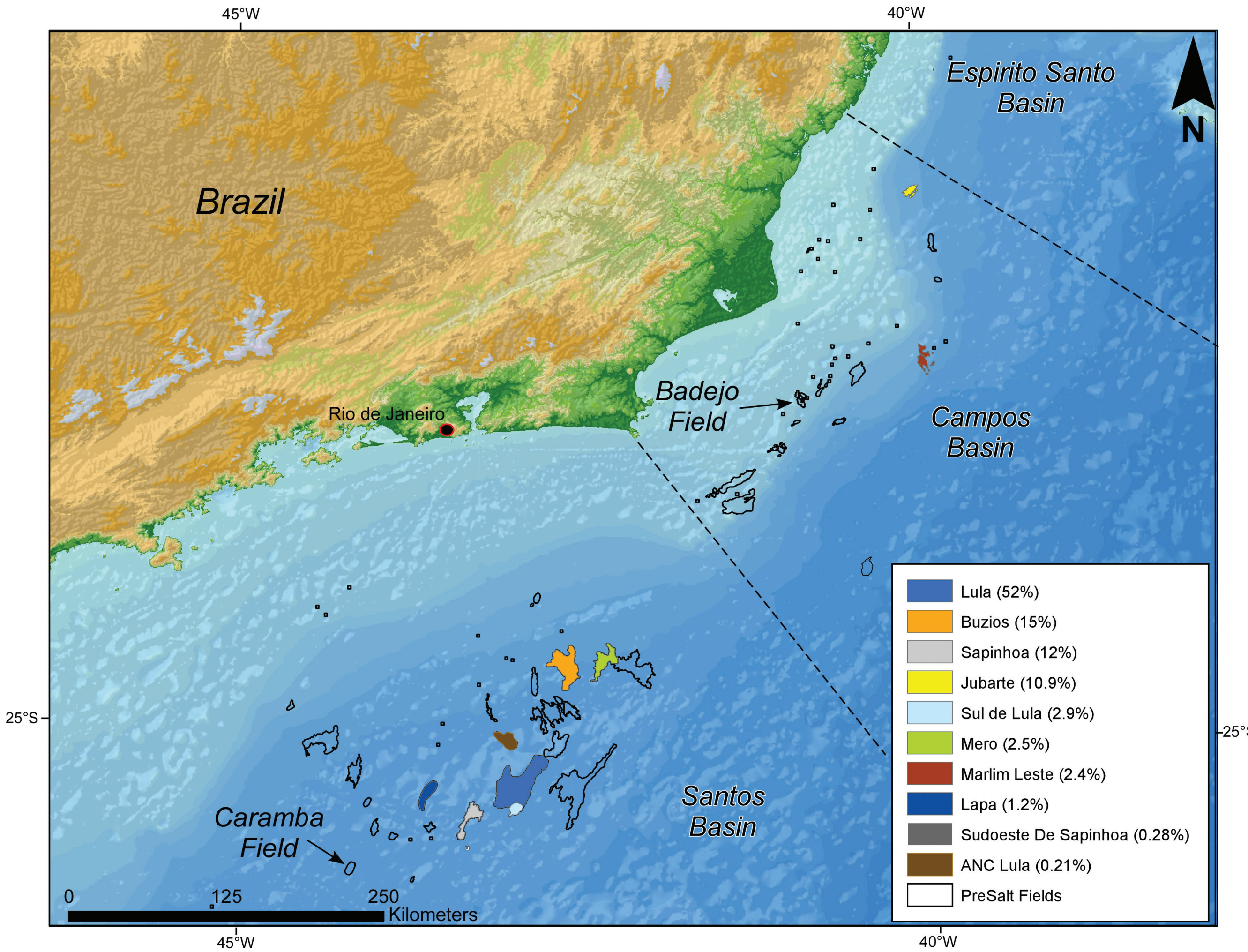

Figure 8. Location and extent of existing pre-salt fields in the Santos and Campos Basins, offshore Brazil. Percentages indicate relative contribution to pre-salt production as at January 2020 (ANP, 2020).

reimaged and merged into a single, contiguous data volume. It was reimaged using a calibrated anisotropic velocity model, and consistently datumed, amplitude balanced, and phase matched. The velocity model was constructed using multiple tomographic iterations constrained by well data and regional interpretation of relevant velocity boundaries, including top Albian carbonates, top Aptian salt, base Aptian salt, and top Lower Cretaceous synrift basement.

3-D Merging and Seismic Reimaging Workflow

The reimaging workflow initiated with state-of-the-art noise attenuation and enhancement techniques. This included ION's WiBand^{TM} deghosting, multimodel adaptive subtraction for surface related multiple attenuation (3-D SRME), and careful survey matching prior to imaging. Figure 10 shows the processing, merging, and reimaging workflow, from navigation-merged raw data to final imagery. The effectiveness of 3-D SRME is shown in Figure 11.

For velocity model building at the scale of the Picanha 3-D seismic volume, gridded tomography, aided by information from hundreds of wells and key seismic surface interpretation, is used. As a starting point, we used a water profile derived from regional temperature/salinity measurements, detailed bathymetry picked on a 25 × 25 m water flood PreSDM stack, and a sediment model derived from ION's 2-D *BrasilSpan* program (Figure 12 [top]). This enabled tomography to capture fine lateral and vertical detail in the post-salt section in only three

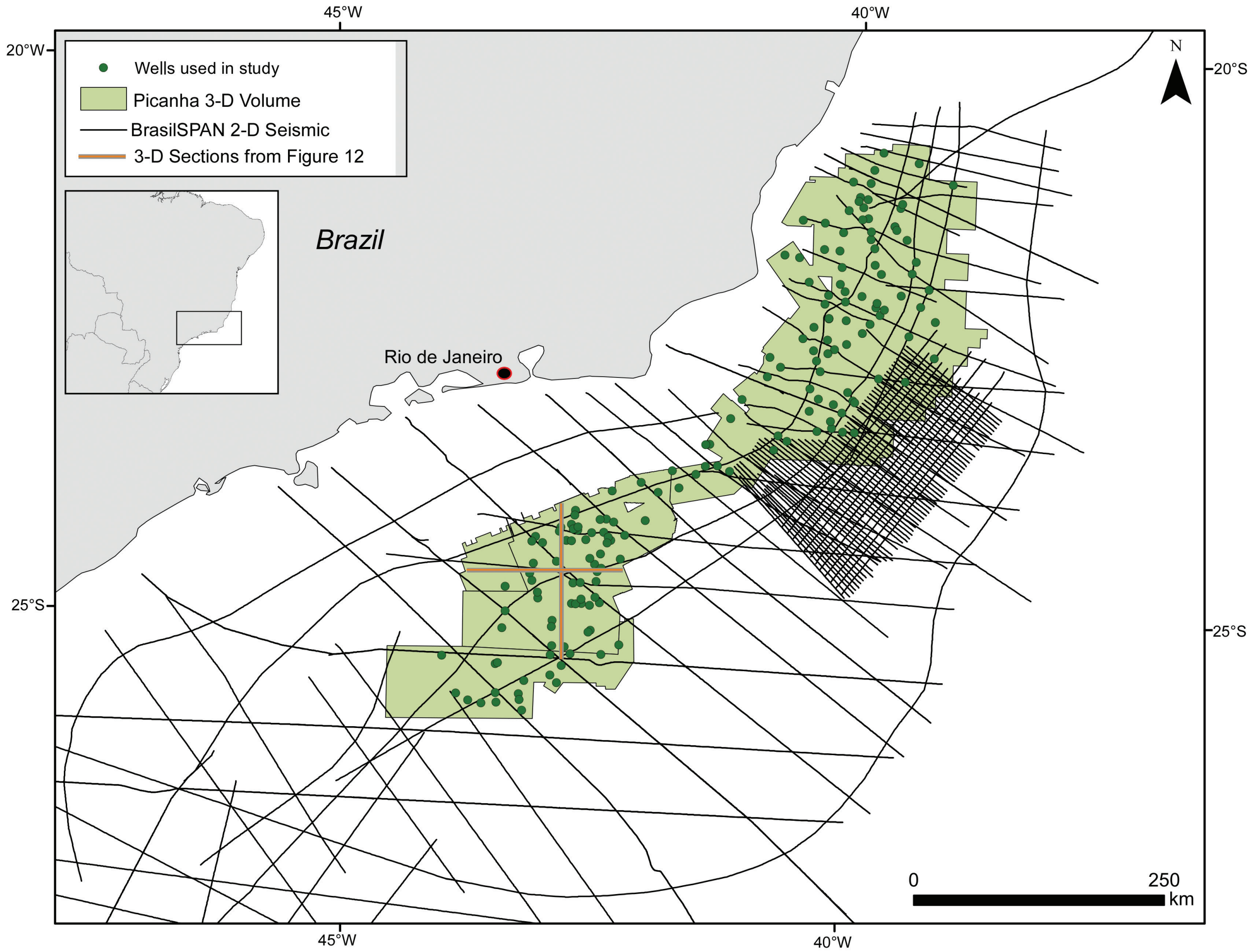

Figure 9. Map showing seismic and well data used for this study.

iterations (Figure 12 [middle]), using inversion cells decreasing from 1 km to as little as 300 m laterally and 50 m vertically. Anisotropy from fourth-order residual moveout picking was then introduced. This approach ensures that vertical and lateral lithologic changes are being reflected in the variability of the anisotropic parameter's delta. Well tops are used to calibrate delta such that the top salt ties within 1% of the well depth and the seismic velocity is a good low-frequency representation of the sonic data. Additionally, the structurally extrapolated sonic logs are used to constrain the tomographic inversion of both velocity and epsilon. Synthetic and seismic tie analyses for several wells confirm the quality of the overburden model (Figure 13).

Interpretation of top and base salt, including overhangs where present, is a crucial part of velocity model building described herein. Where applicable, the top of the high-velocity Albian carbonates is used to limit anisotropy to the overburden sediments. In contrast to much of the Campos Basin, the salt in the Santos Basin shows strong intra-salt reflectivity. As a localized and separate study, velocity variability with both tomography and FWI is successfully captured. For the purpose of the basin-wide image discussed here, a constant average salt velocity of 4500 m/s was sufficient to flatten the base salt reflection optimally. In the hydrocarbon-relevant pre-salt, tomography captured velocity variations associated with the high-amplitude sag sediments (Figure 12 [bottom]). Below this level, a gravity-derived crustal velocity trend is used to image beneath basement to a depth of 15 km.

Processing, Merging, and Reimaging Workflow

1. **Data Preparation**
    - Debubble
    - Denoise
    - Deghosting
    - Zero-phasing
2. **Multiple Attenuation**
    - Short-period 3-D SRME
    - High-Resolution Radon
3. **Survey Matching/Regularization**
4. **Anisotropic Velocity Model Building**
    - TTI and gridded tomography, constrained by sonic, density, check-shot data from 174 wells, and velocity interface/geologic layer interpretation
5. **PSDM Imaging**
    - Model-building units
        - Water column
        - Water bottom to top Albian
        - Top Albian to top salt
        - Top salt to base salt
        - Base salt to basement
    - Gravity-data-constrained velocity gradient from top basement to MOHO
6. **Post Processing**

Figure 10. 3-D data processing, merging, and reimaging workflow.

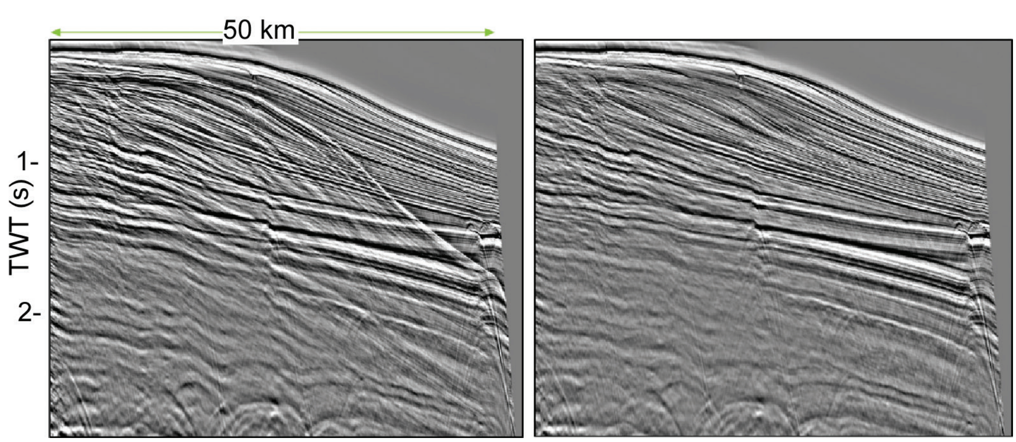

Figure 11. Full stack before and after 3-D Surface Related Multiple Elimination (SRME) showing de-multiple effectiveness in shallow water, which is crucial for residual move-out picking prior to tomography.

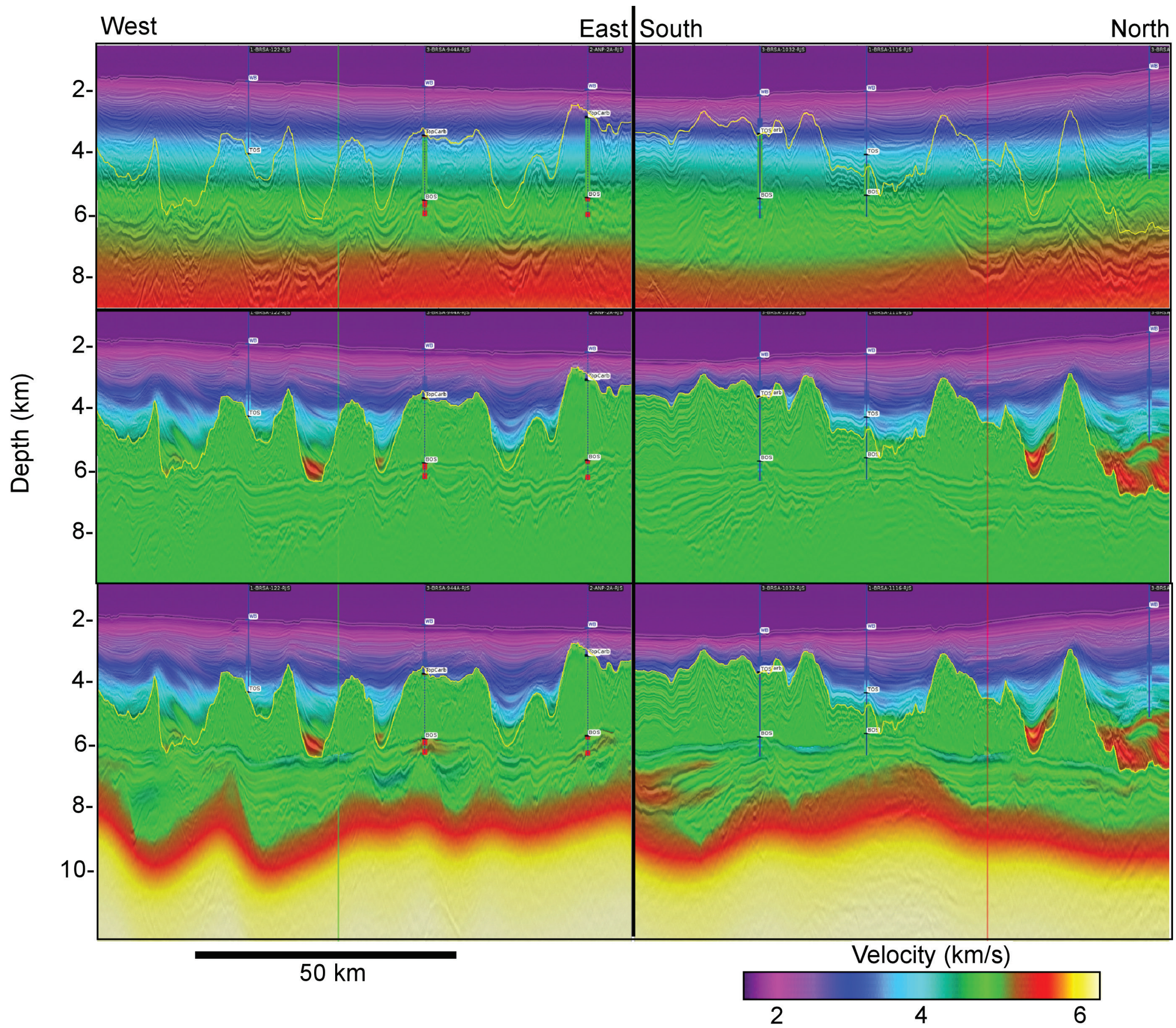

Figure 12. Santos Basin inline (left) and crossline (right) co-rendered with an initial velocity model from the 2-D *BrasilSPAN* program (top), post-salt sediment model after three tomographic iterations (middle), and final model showing a detailed image of the hydrocarbon-relevant syn-rift and post-rift sag sections and the deeper crustal structure (bottom). Line locations are shown on Figure 9.

THE SANTOS BASIN PRE-SALT (PICARRAS AND ITAPEMA) PETROLEUM SYSTEM

The Santos Basin pre-salt petroleum system is contained within the Barremian-to-Aptian synrift to post-rift sag sequences (Figure 5). The Santos Basin petroleum system is a supercharged system. As such, most traps are filled to spill, and oil column heights vary with closure height. As demonstrated at Sepia Field, Santos Basin thick salt seals can contain oil columns greater than 600 m in height.

Pre-Salt Source Rocks

The principal source rocks of the Santos Basin are lacustrine shales of the upper Barremian (Jiquiá stage) Itapema Formation and, to a lesser extent, the lower Barremian Picarras Formation (Mello et al., 2020). Most giant fields in the Santos Basin are charged from upper Barremian Itapema calcareous shales (Mello et al., 2020). The Itapema Formation is correlative with Coqueiros Formation of the adjacent Campos Basin.

Itapema Formation organic matter is lipid rich, of algal and bacterial origin, and contains lacustrine hydrogen-rich oil-prone kerogen. Santos Basin pre-salt oils are nonbiodegraded, as temperatures at reservoir depths far exceed those conducive to microbial degradation. Source rock maturation relates to burial of the lacustrine shales under a thick succession (locally greater than 5 km) of post-rift sediments. Peak oil generation likely initiated in Upper Cretaceous time and migration continues today (Kemna et al., 2021).

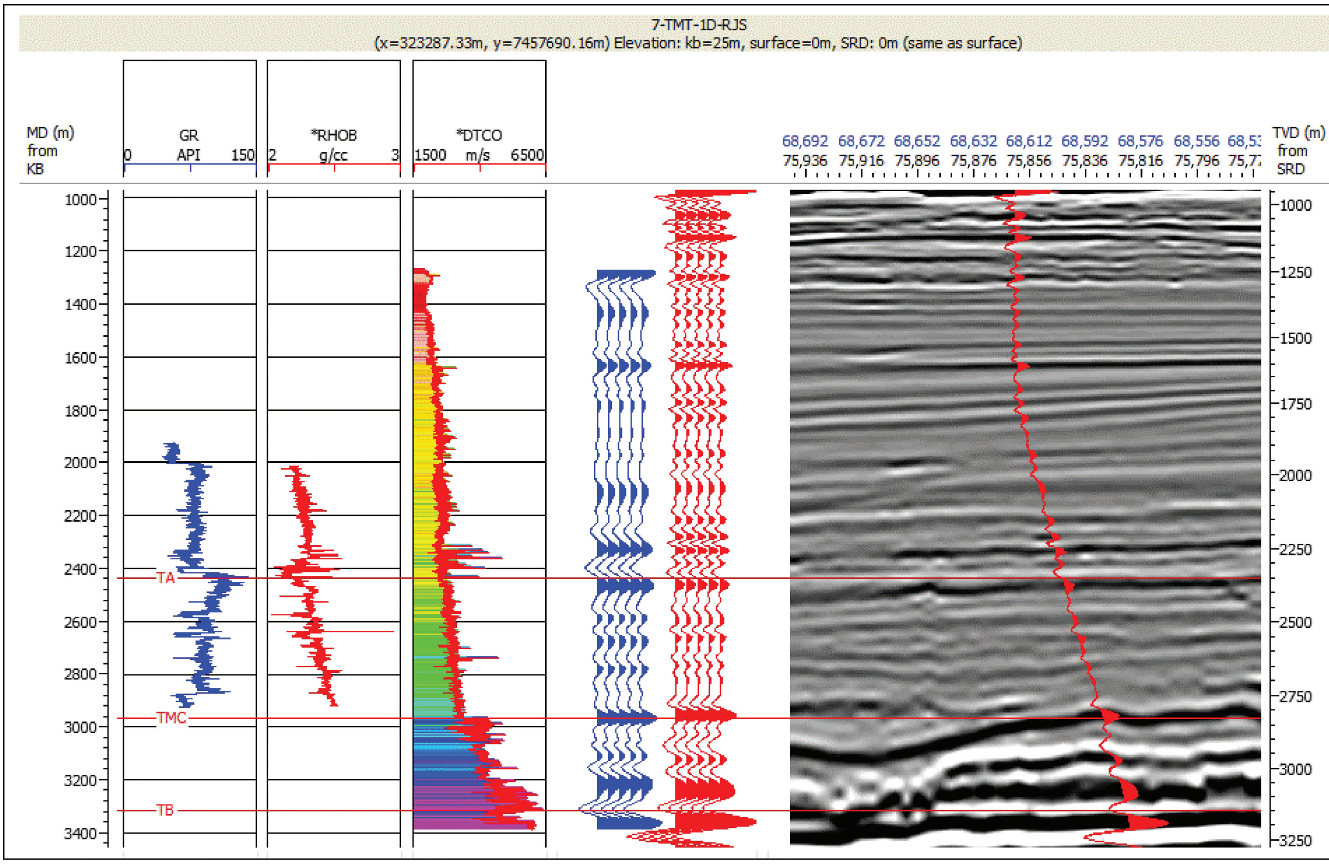

Figure 13. Synthetic seismogram showing a good match with seismic data at all levels from water bottom to top salt.

Analysis of diamondoids in oil samples from deep and ultra-deep Santos Basin wells suggests the presence of mixed oils, representing multiple phases of charging and mixing of noncracked ("black") oil with highly cracked oil (Mello et al., 2020). Mello et al. (2020) postulate that cracked oils migrated from an outboard thermally overmature kitchen on the eastern flank of the Santos Basin Outer High. These oils are mixed with noncracked ("black") oils sourced from a kitchen west of the Santos Basin Outer High. The coexistence of both cracked and noncracked oils at Tupi and Jupiter fields is consistent with this theory (Figure 5; Mello et al., 2021; Dahl et al., 2021).

Pre-Salt Reservoirs and Reservoir Fluids

Pre-salt reservoirs of the Barra Velha Formation comprise lacustrine mollusk coquinas disconformably overlain by lacustrine microbialites. Microbialites comprise microbialite shrubs, stromatolitic microbialites, microbial mats, wackstone/packstone spherulites, grainstones, mudstones, and travertine (Ceraldi and Green, 2016). On the Santos Basin Outer High, the units are separated by an interval of shale and argillaceous/arenitic carbonates 15–20 m thick.

The lacustrine carbonate reservoir package, comprising coquinas and microbialites, is commonly 500–600 m thick. The thickness of the individual lithologies is dependent on their paleodepositional position and proximity to the lakeshore. Pre-salt coquinas are widespread and extend hundreds of kilometers from the southern Santos Basin northward into the Campos Basin. Microbialite deposition, however, is more restricted, because of local variations in post-rift geomorphology and post-rift thermal subsidence.

Moldic, intergranular, intercrystalline, and fracture porosity are characteristic of both reservoir facies (Corbett, 2015). Mineralogically, pre-salt carbonates are composed principally of calcite, dolomite, and silica, with varying amounts of magnesium-rich clays, such as stevensite, and heavy minerals, such as pyrite (Boyd et al., 2015).

Pre-salt reservoirs are characterized by moderate porosity and high permeability, the latter resulting in exceptionally high well deliverability. At Buzios Field, for example, porosity ranges from 10% to 18% and effective permeability (to oil) ranges up to 5 darcys (Petersohn et al., 2013). Kv/Kh typically is on the order of 0.1 (Elias et al., 2014). The Buzios discovery well (2-ANP-1-RJS) flowed at an initial rate of 50,000 BOEPD from the Barra Velha Formation (Offshore Technology, 2018). The seven most prolific Buzios development wells have produced at rates ranging from 35,849 BOPD (7-Buz-29D-RJS) to 50,843 BOPD (7-Buz-29D-RJS; Avila, 2017; ANP Bulletin, 2020). In 2019, more than 45 Santos Basin pre-salt wells individually were producing more than 15,000 BOPD (ANP Bulletin, 2020; Figure 3).

On the Santos Basin Outer High, pre-salt reservoirs are slightly overpressured (0.5 psi/ft gradient) and are undersaturated at initial reservoir conditions. One known exception is the Jupiter discovery, which is saturated at initial reservoir conditions and has a free gas cap. Regionally, the degree of overpressuring decreases from west to east (N. Maden, personal communication, 2020).

Rock and fluid expansion are principal primary recovery drive mechanisms as fields are drawn down to bubble-point pressure. Solution gas drive dominates from bubble-point pressure to abandonment pressure, with the assistance of water injection as a means of secondary recovery. Bubble-point pressure (Pbp) is 7,190 at 100°F (Boyd et al., 2015).

Because of the high thermal conductivity of the salt, reservoir temperatures are anomalously low given overburden thickness. Temperatures range from approximately 90°C to 105°C (Boyd et al., 2015). On the Santos Basin Outer High, pre-salt oil API gravity ranges from 27° to 39° (Petersohn et al., 2013). At Tupi Field, downhole oil viscosity is approximately 1 cP (Boyd et al., 2015). It contains 0.1% CO_2, 0.3% sulfur, and minor amounts of H_2S. Initial GOR is 380–395 scf/stb (Boyd et al., 2015). Associated gas contains 8%–18% CO_2 (Formigli et al., 2009).

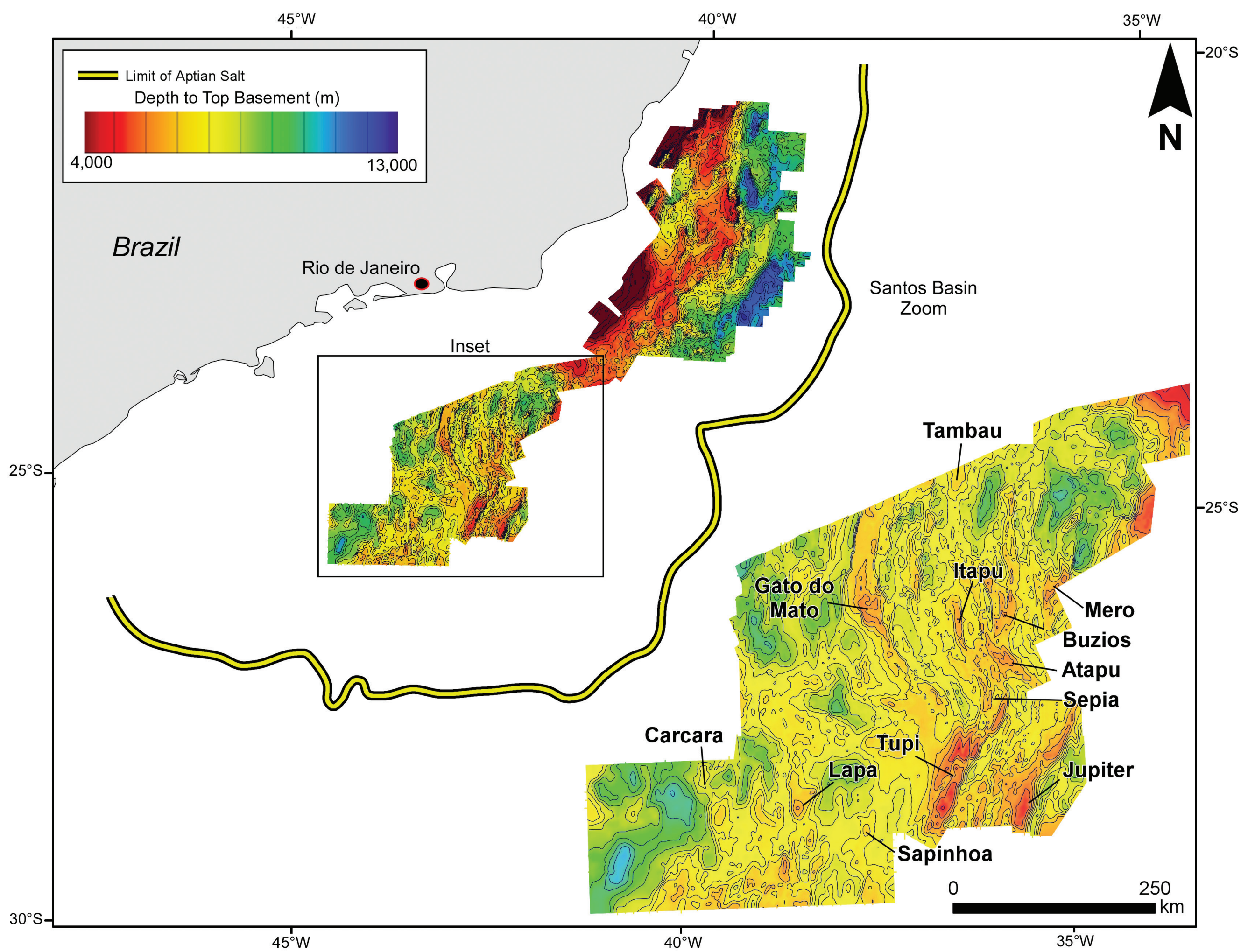

Figure 14. Top-basement depth structure map**,** Santos and Campos Basins. Note the association of multi-billon-barrel pre-salt fields with basement highs.

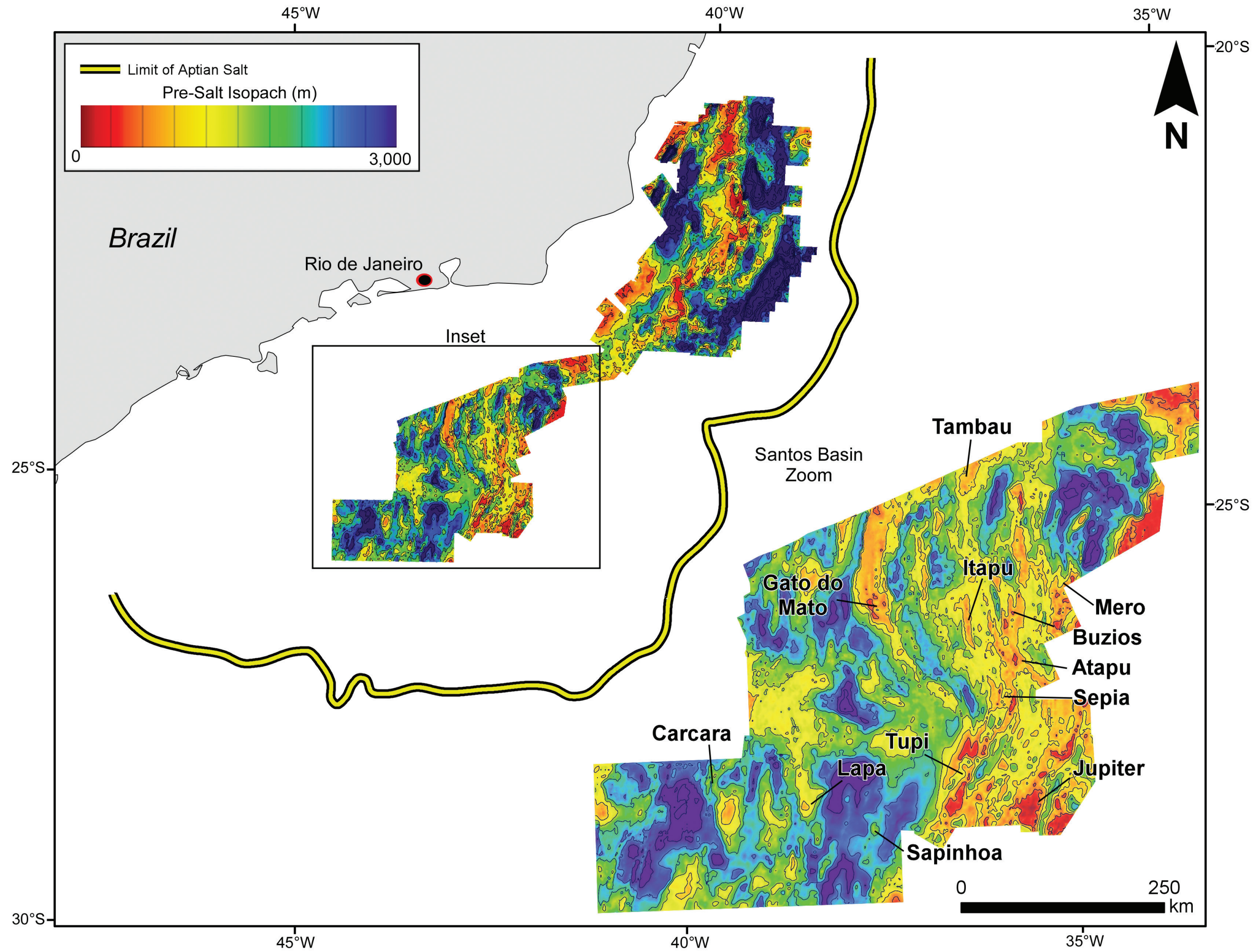

Figure 15. Pre-salt isopach map (base-salt to top-basement). Note the association of Santos Basin pre-salt fields with pre-salt isopach thins.

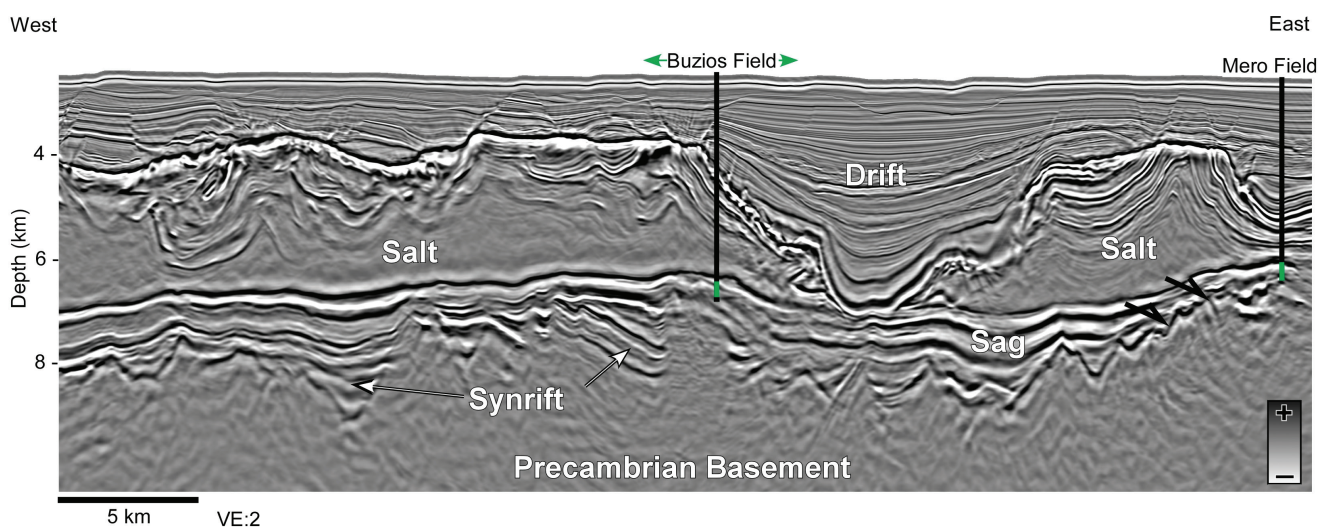

Figure 16. PSDM seismic transect through Buzios Field, a complex four-way-dip structural closure, showing: dip closure at base-salt (top-reservoir) level; a thick (>2 km) overlying salt seal; and fault-bounded, rotated half-graben containing syn-rift growth strata disconformably overlain by post-rift sag reservoirs.

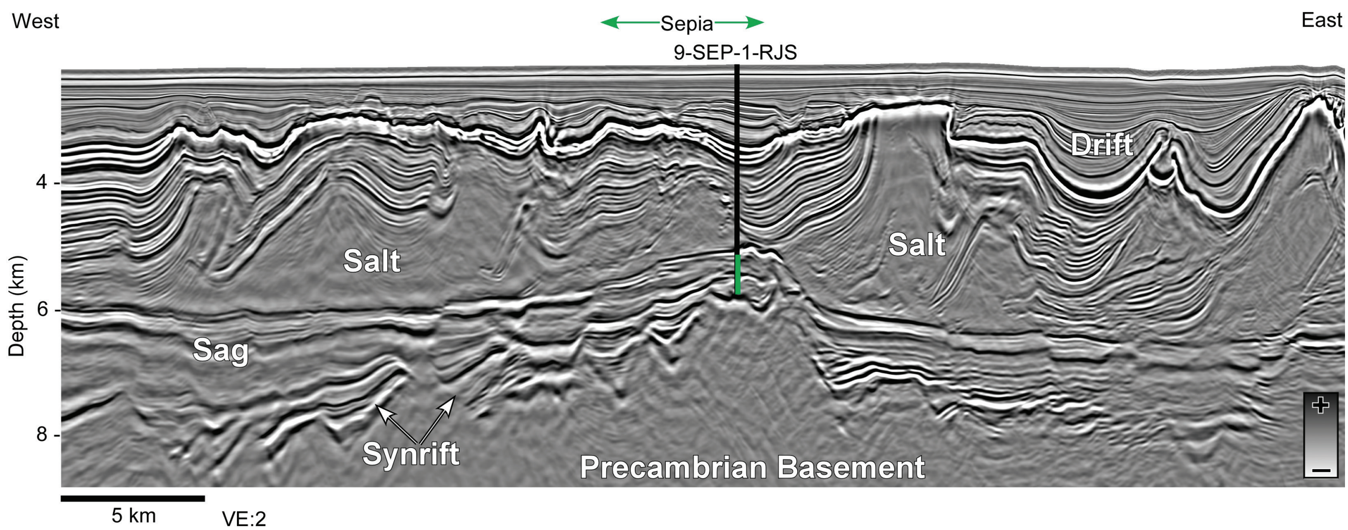

Figure 17. PSDM seismic transect through Sepia Field, a three-way dip closure. Reservoirs are sealed updip by juxtaposition with Aptian salt along a high-angle, basement-involved normal fault.

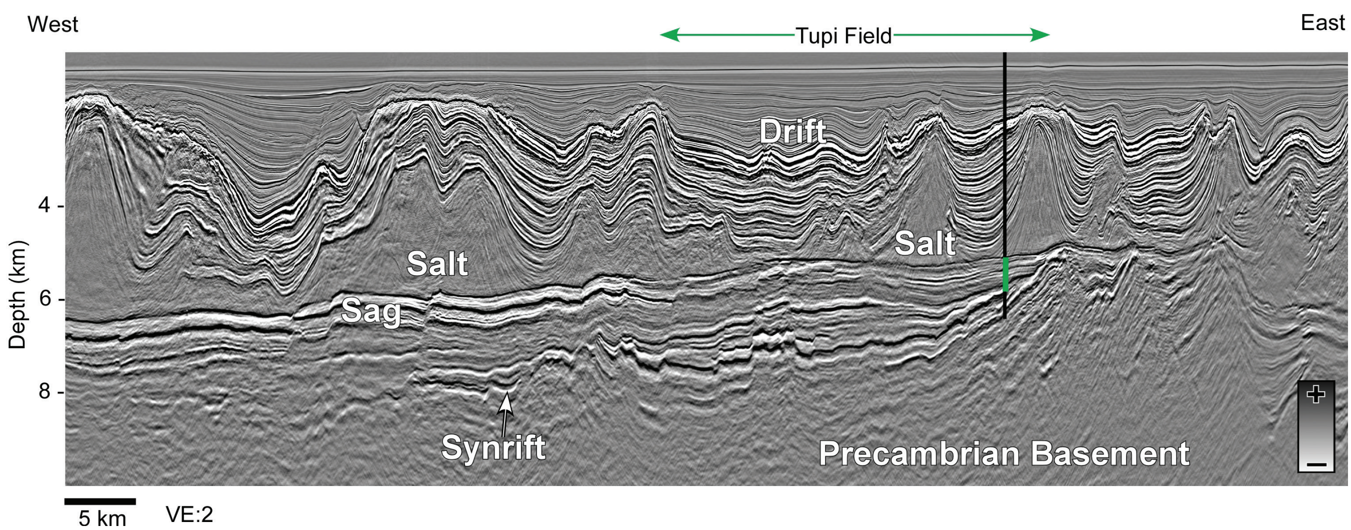

Figure 18. Regional PSDM seismic transect through Tupi (Lula) Field, Brazil's largest pre-salt oil and gas field. Note onlap of post-rift sag strata onto syn-rift, fault-bounded, rotated fault blocks; the regional base salt structural high; a layered evaporite top seal 2 km thick; and the west-to-east decrease in Acoustic Impedance (increase in porosity) beneath the base-salt horizon.

The outer (eastern) Santos and Campos basin kitchens are thought to be the source of the CO_2 (Figure 19). Consistent with this, the CO_2 content of Jupiter Field is anomalously high: sampled gas contains 75 mole percent CO_2; recovered oil contains 55 mole percent CO_2 (Mello et al., 2020). Other hydrocarbon accumulations with direct access to the outer kitchens are equally likely to have elevated CO_2 content.

Although the presence of CO_2 can be explained locally by volcanic plumes and seamounts, in the eastern Santos Basin, elevated CO_2 may be because of mantle degassing along crustal strike-slip faults. This late-stage CO_2 has a significant negative impact on crude oil quality (N. Maden, personal communication, 2020).

Pre-Salt Seals

Santos Basin pre-salt petroleum accumulations are sealed by a locally thick (>2 km) mobile sequence of Aptian evaporites, principally halite and anhydrite, interbedded upsection with fine-grained clastics and carbonates. The Santos Basin halokinetic style is one of the dominantly passive, load- and gravity-induced, autochthonous salt deformation and translation. In some areas on the Santos Basin shelf, the salt is entirely evacuated. Although allochthonous salt canopies occur in the far eastern parts of the Campos and Santos Basins, detached salt bodies are relatively rare. In this respect, the Santos Basin differs considerably

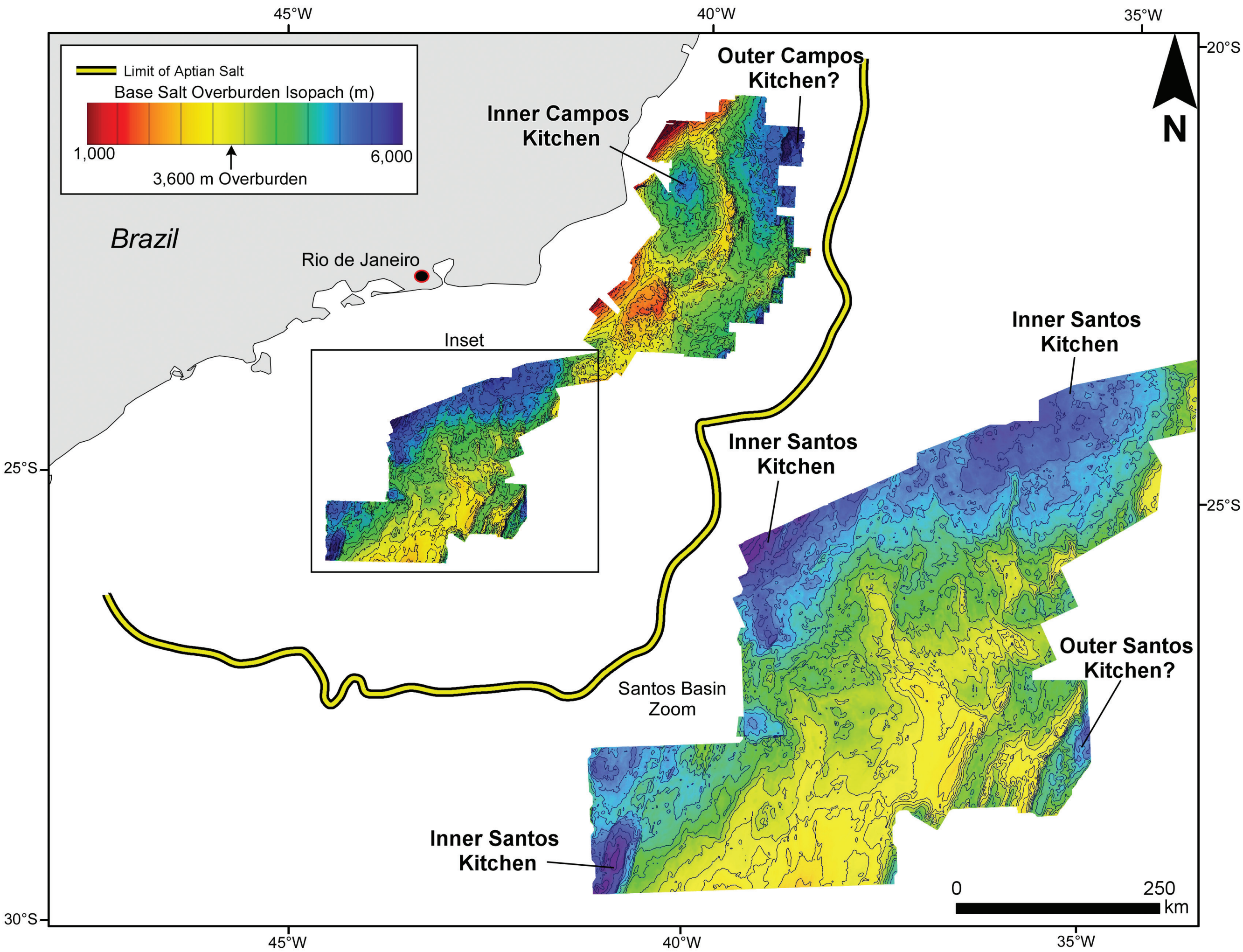

Figure 19. Base-salt overburden map, a proxy for top-Itapema source rock burial depth. Note the "Inner Santos kitchen" inboard (west and north) of the Santos Basin Outer High, a possible "Outer Santos kitchen" outboard (southeast) of the Santos Basin Outer High, and inboard and possible outboard kitchens in the northern Campos Basin.

from other salt provinces such as the U.S. and Mexican Gulf of Mexico (Pindell et al., 2015).

There are no known significant pre-salt petroleum accumulations lacking a salt seal in the Santos Basin.

Pre-Salt Trapping Styles

Pre-salt oil and gas accumulations are commonly trapped in complex, faulted, sub-salt four-way-dip structural closures with multiple structural culminations. They commonly associate with basement highs (Figure 14) and pre-salt isopach thins (Figure 15). Buzios (formerly "Franco" Field) and Sepia fields are notable examples (Figures 16, 17).

Sepia Field is contained in a three-way-dip structural high, closed updip by a basement-involved normal fault that juxtaposes pre-salt reservoirs with Aptian salt (Figure 17).

Tupi Field, one of the largest oil and gas field in Brazil, displays a strong element of stratigraphic trapping, with post-rift sag reservoirs unconformably onlapping a synrift high (Figure 18).

IMPLICATIONS FOR PRE-SALT PETROLEUM EXPLORATION

Pre-Salt Play Fairway Mapping

The Santos Basin pre-salt play fairway is herein defined as that area in which all elements essential to accumulation of pre-salt (Itapema coquina and/or Barra Velha microbialite) hydrocarbons spatially overlap. These

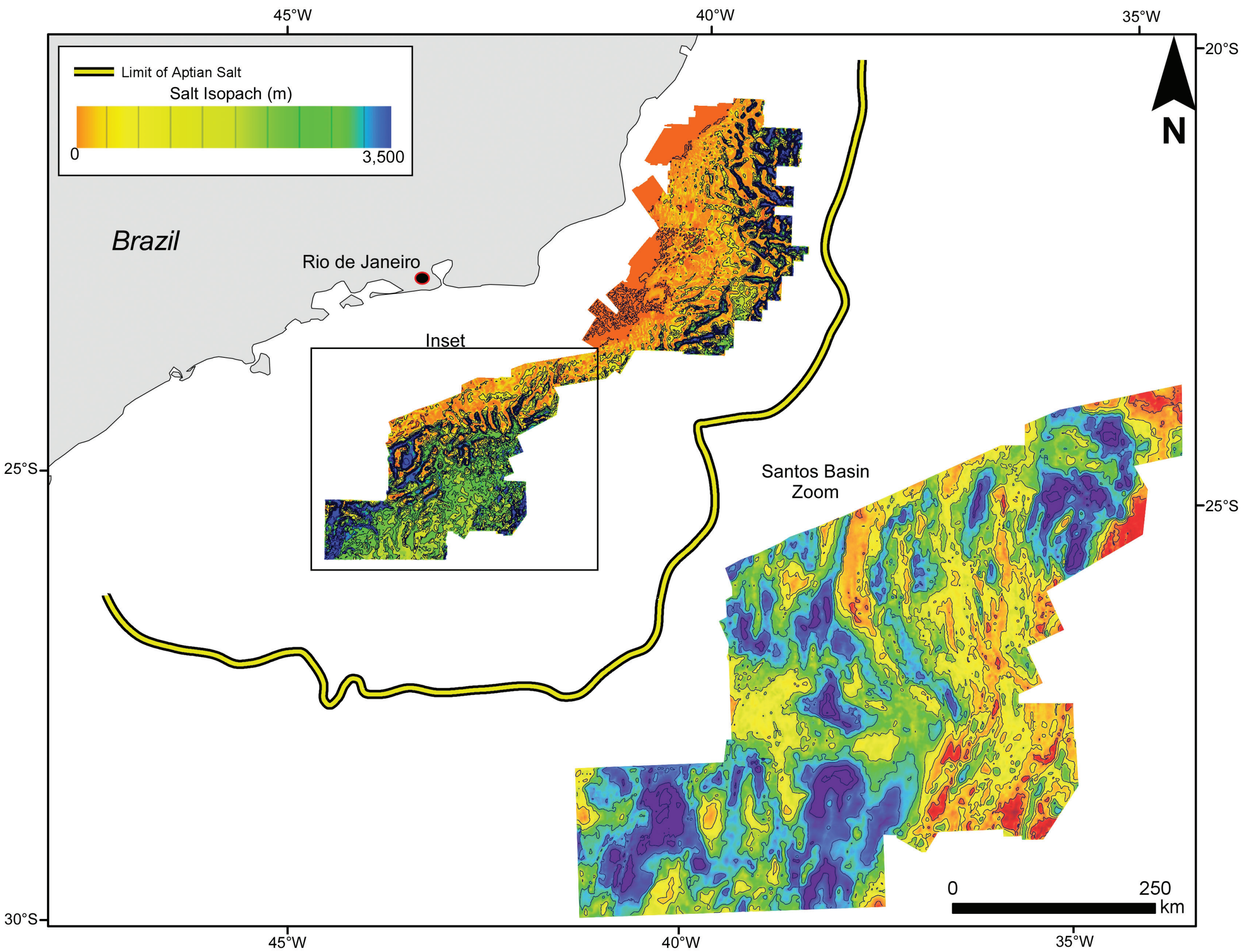

Figure 20. Distribution and thickness of the Ariri Formation salt seal in the Campos and Santos Basins, within the Picanha 3-D reimaging area. Note: (1) the presence of thick mobilized salt in the Santos Basin and deep-water Campos Basin; and (2) relatively thin salt on the Santos and Campos Basin shelves.

elements include source presence and effectiveness, seal presence and effectiveness, and reservoir presence and effectiveness. The play fairway may extend beyond the area of spatial overlap where carrier beds enable lateral hydrocarbon migration to areas outside of the area of present-day source rock thermal maturity. An area of Santos Basin pre-salt prospectivity is defined using this play fairway mapping methodology.

Common risk segment mapping, a method in which different levels of risk are assigned to each play fairway component and then spatially combined, was not carried out.

Source Presence and Effectiveness

The position of COB controls the east/southeastern (basinward) limit of the synrift sequence, hence synrift source rock deposition. Inboard of the COB, source rock thickness and distribution are related to the location and degree of crustal extension, hence half-graben development, resulting in conditions conducive to source rock deposition. Basement architecture, and reactivation of preexisting basement faults, possibly associated the Ribeira fold belt (K. R. Reuber, personal communication, 2020), could be important controls on graben development.

Santos Basin present-day source rock thermal maturity relates to many factors, including kerogen kinetics, heat flow (dependent largely on crustal type and salt thermal conductivity), rifting history, and source rock burial history. Although burial history modeling is not a part of this study, available seismic data enable delineation of crustal types and source rock overburden. The latter, using the base salt surface as a proxy for top source rock, is shown

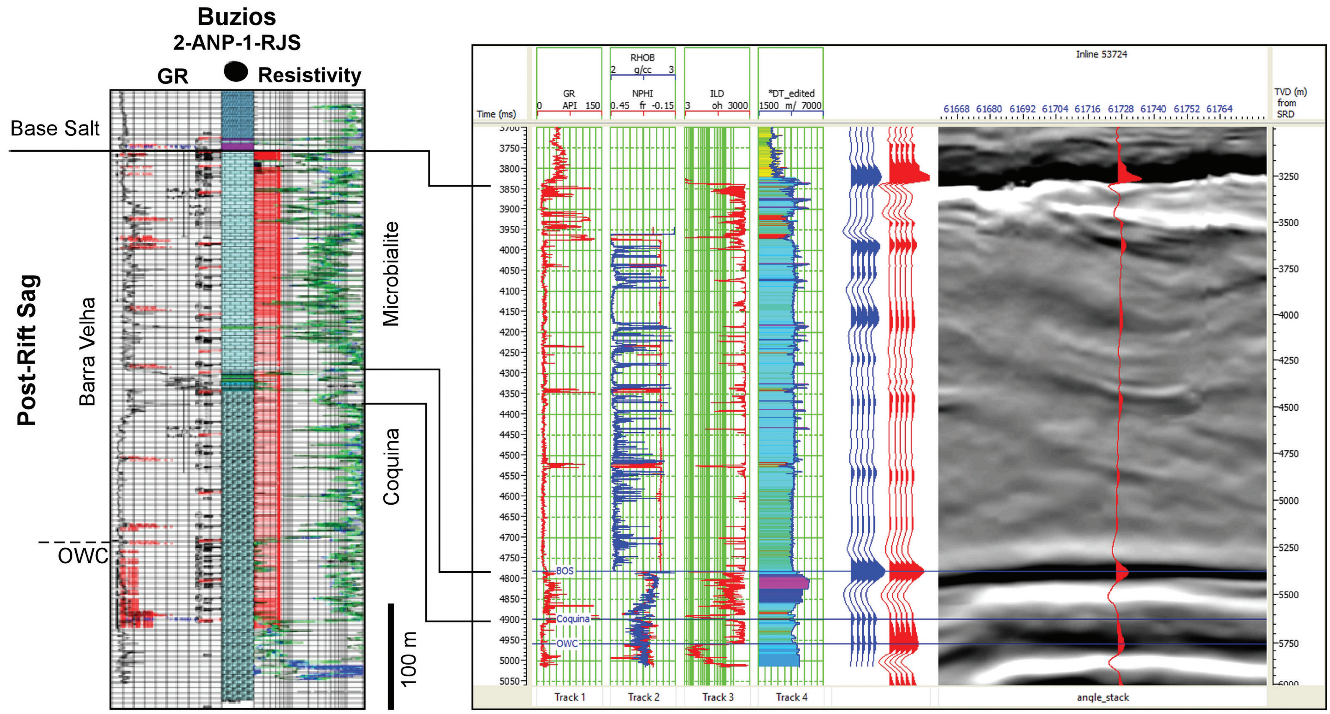

Figure 21. Full-stack PSDM seismic expression of microbialite and coquina reservoirs at Buzios Field, Santos Basin.

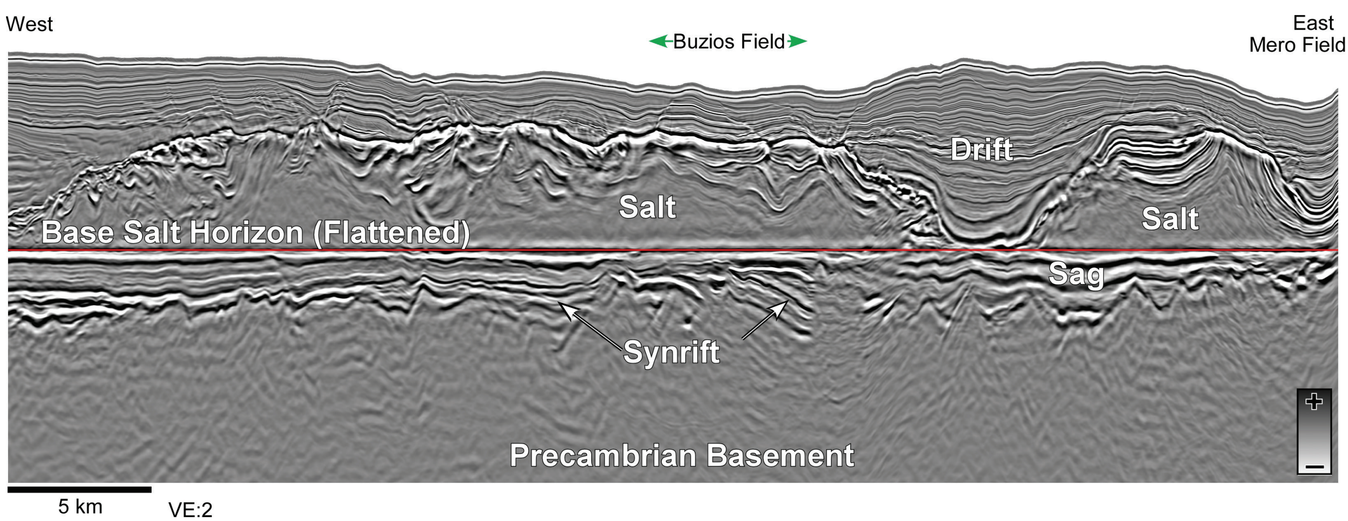

Figure 22. Regional PSDM transect through Buzios Field flattened at the base-salt horizon to approximate depositional architecture at the end of post-rift sag deposition. Note the eastward thinning of the post-rift sag (thermal subsidence) sequence onto the Buzios structure.

on Figure 19. This map defines kitchen areas inboard and outboard of the Santos Basin Outer High and inboard and outboard kitchen areas in the northern Campos Basin.

Santos Basin geothermal gradients range from 24ºC/km to 41ºC/km (Cardoso and Hamza, 2014). Assuming that the onset of oil generation occurs at approximately 100ºC, at least 3300 m of base salt overburden is required for oil generation. M. Mello (personal communication, 2020) indicates that 3600–4200 m of overburden is required for the onset of oil generation in the Santos Basin. Using a 3600 m overburden threshold, general pre-salt kitchen areas can be defined (Figure 19). Within these kitchens, kerogen

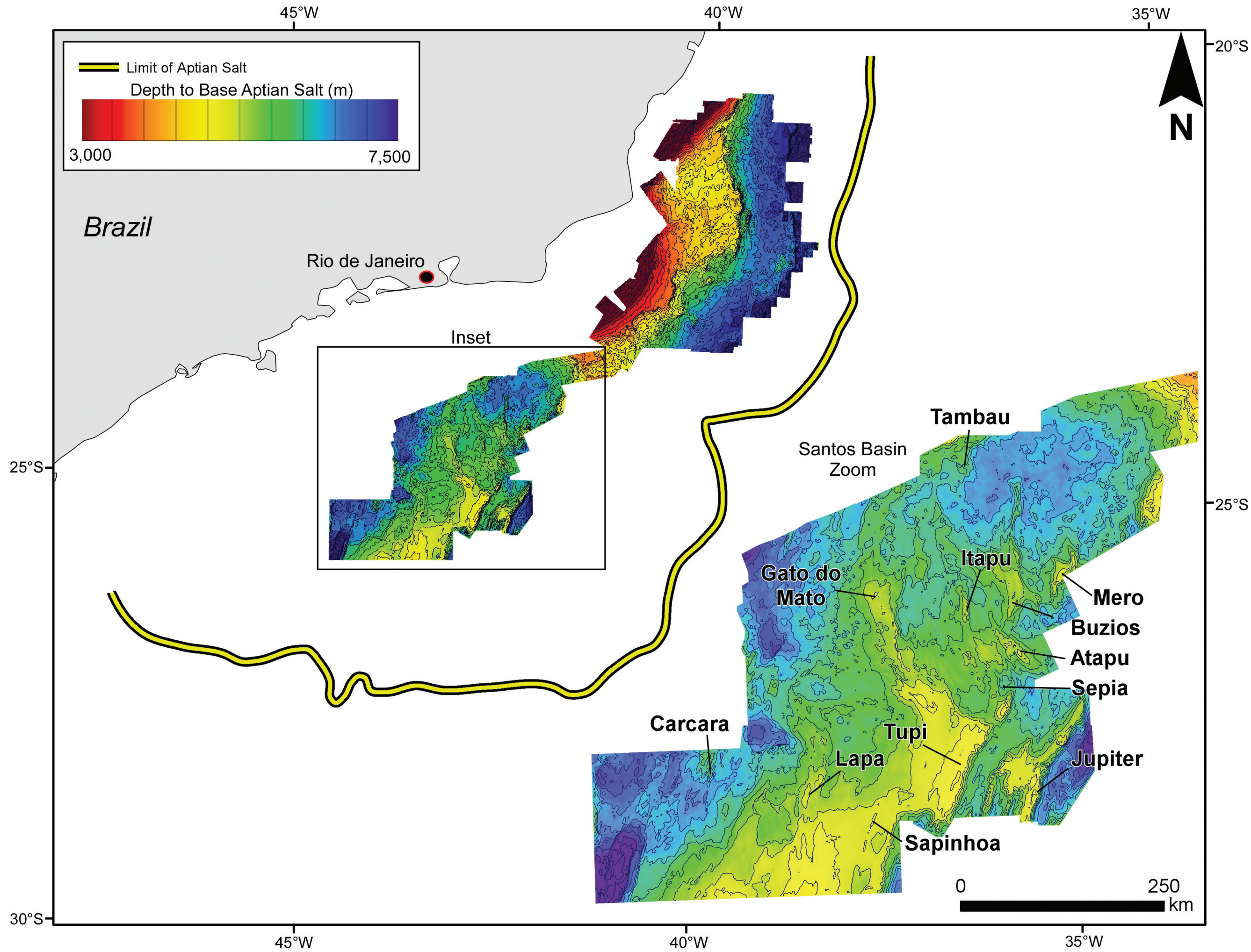

Figure 23. Base-salt (top Barra Velha reservoir) depth structure map. Note the association of multi-billion barrel pre-salt fields with base-salt structural highs, and the many undrilled structural culminations.

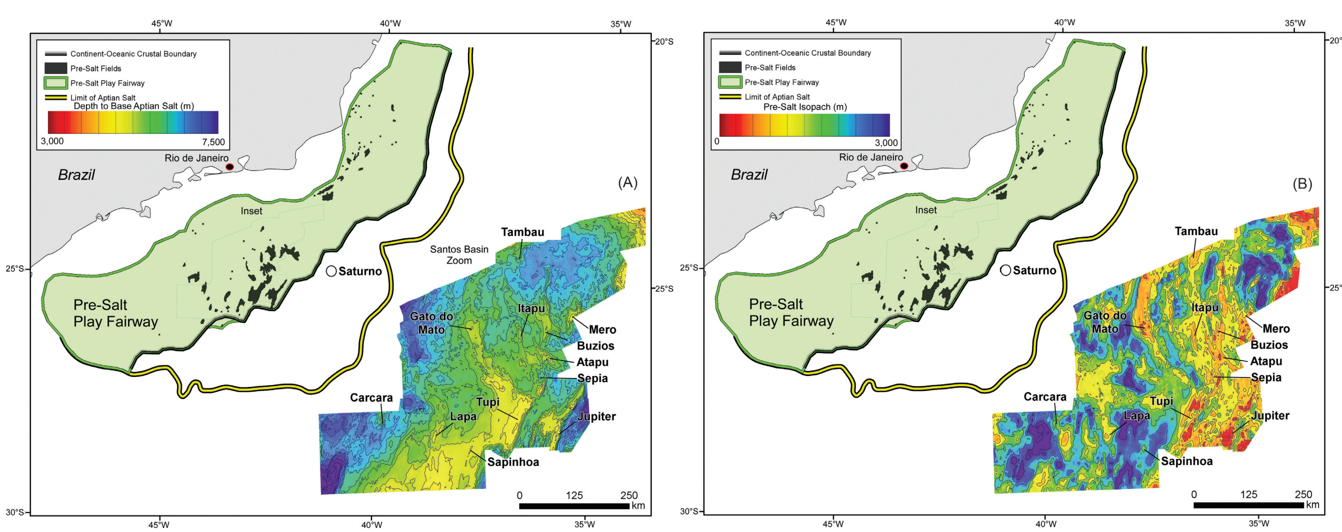

Figure 24. Generalized Santos and Campos Basins pre-salt (Barra Velha Formation) play fairway, shaded in green, with a base salt (top reservoir) depth structure inset (a) and a pre-salt isopach inset (b). Note the location of the Saturno dry hole, drilled outside of the play fairway in 2020.

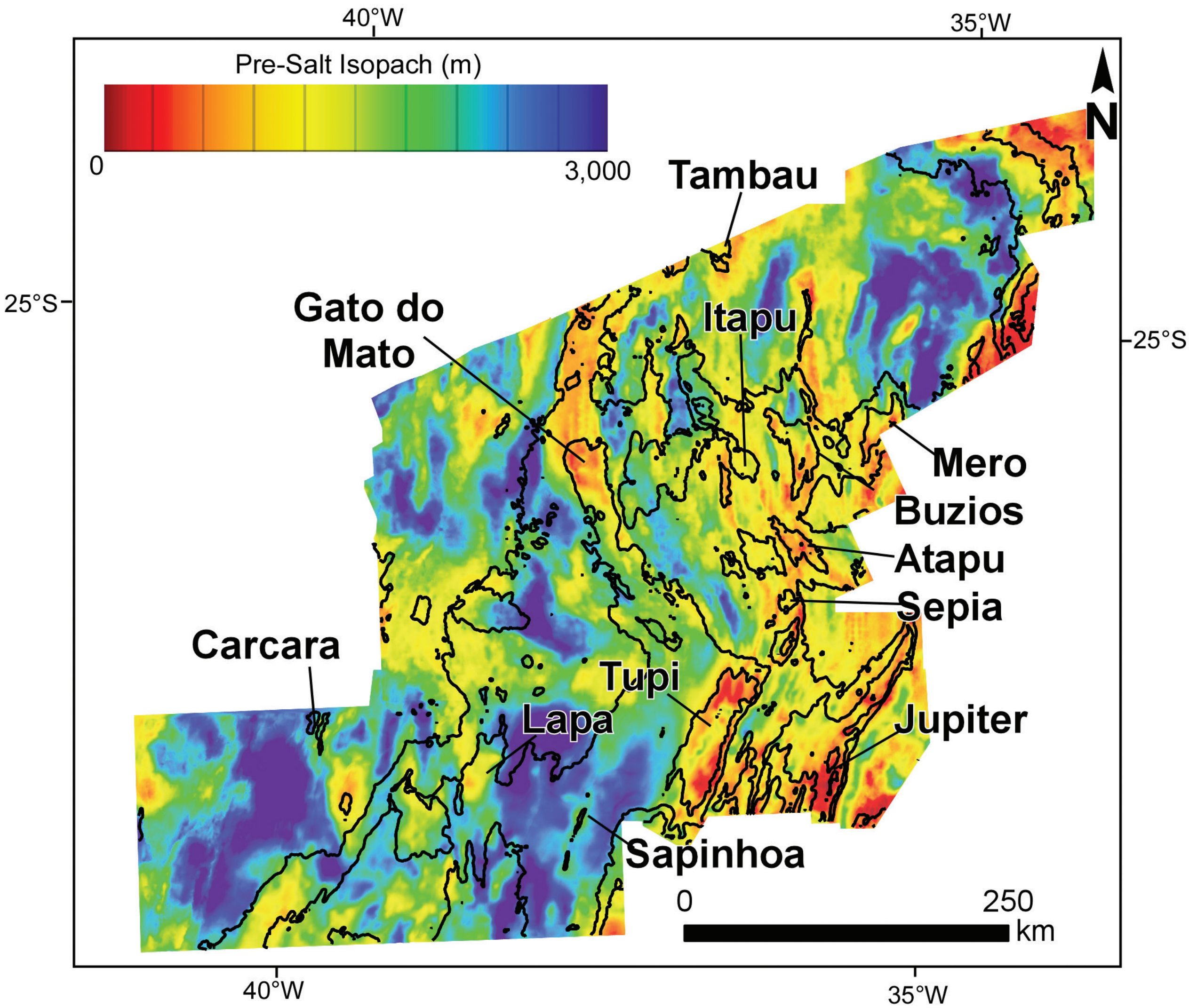

Figure 25. Base-salt/top reservoir depth structure (contours) superimposed on a pre-salt isopach (color fill). Note the association of Santos Basin Outer High pre-salt fields with both base-salt structural highs and pre-salt thins.

facies variation is expected; therefore, expelled hydrocarbon type (gas/oil) is unknown.

Seal Presence and Effectiveness

The thickness and distribution of the Aptian salt seal is well defined in the study area (Figure 20). The Aptian salt seal is known to hold 26° API (Sg = 0.898 at 60°F) oil columns greater than 600 m in height. In these areas, salt thickness typically exceeds 2000 m. Salt welds occur locally throughout the basin (Figures 14–16). At salt welds, seal risk is expected to be high, unless the post-salt sequence contains a significant thickness of high-clay-content strata. No pre-salt petroleum accumulations are known to exist in such areas.

Reservoir Presence and Effectiveness

Barra Velha Formation coquina reservoirs are widespread. Well data indicate that they extend through hundreds of kilometers from the deep-water southern Santos Basin (e.g., Caramba Field) to the Campos Basin shelf (e.g., Badejo Field) and northward to the deep-water Campos Basin Jubarte Field (Figure 8). With adequate well control, coquina reservoirs can be discerned seismically from overlying microbialite reservoirs (Figure 21). Regionally, however, in the absence of such well control, the two cannot be distinguished with confidence.

The base salt–to–top-basement interval is mapped in this study, without differentiating synrift strata from post-rift sag strata. We expect post-rift sag (Barra

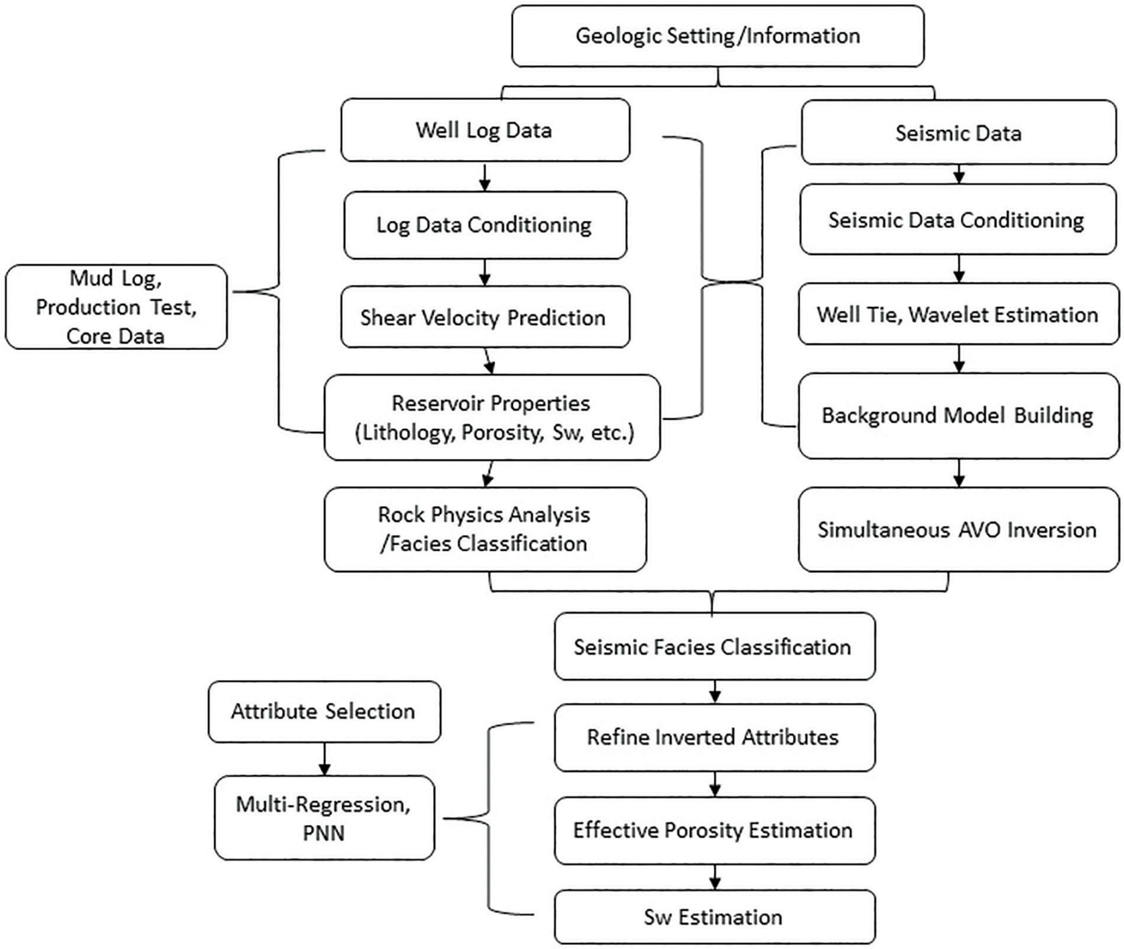

Figure 26. An integrated workflow for Buzios Field pre-salt reservoir characterization.

Velha) reservoirs to thin over preexisting paleotopographic (synrift and basement) highs and to thicken in areas of relatively greater thermal subsidence (Figure 22).

Trap Presence and Effectiveness

Pre-salt hydrocarbon traps, as described earlier, are present throughout the Santos and Campos basins. Pre-salt traps comprise four-way-dip structural closures, fault-bounded three-way-dip structural closures, and three-way-dip structural closures onlapping synrift or basement structural highs.

The Santos Basin Outer High contains multiple base salt culminations that host the Santos Basin's giant oil and gas fields (Figure 23). The largest culmination is the Tupi structure, a broad feature with a gently dipping west flank that provides direct access to the inner Santos kitchen. It contains a steeply dipping east flank, like Jupiter and Sepia fields. This area, which comprises the Santos Basin Outer High, is well positioned to access charge from the west, north, and possibly east.

In the Campos Basin, a cluster of closures is present in the Campos Basin ultra-deep water, due east of Cabo Frio. Many isolated base salt structural closures also are present on the Campos Basin outer shelf.

Resulting Pre-Salt Play Fairway

The pre-salt play extends from the southern Santos Basin northward to the Campos and Espirito Santo basins, through an area of approximately 210,000 km^2 (Figure 24).

The inboard (western) extent of the pre-salt play fairway is controlled by the limit of the Aptian salt seal. In areas where salt is absent, pre-salt

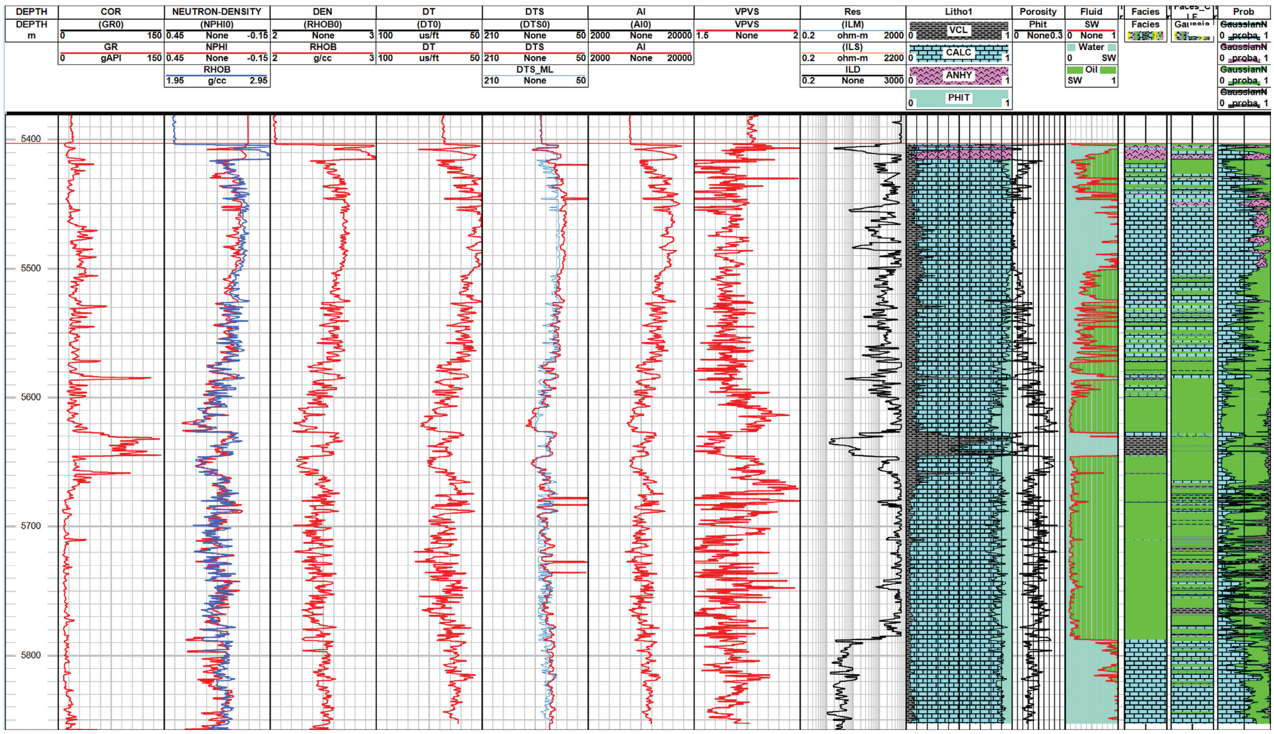

Figure 27. Wireline-log data and interpretation of pre-salt Barra Velha reservoirs at the Buzios Field discovery well (2-ANP-1-RJS). From left to right are: gamma-ray, neutron-density, density, sonic, shear sonic, Acoustic Impedance, Vp/Vs ratio, and resistivity logs. To the right of that are interpreted lithology, porosity, fluid saturation, and lithofacies. In the shear sonic track, measured data are in red; modeled data from data analytics (machine learning) are in blue.

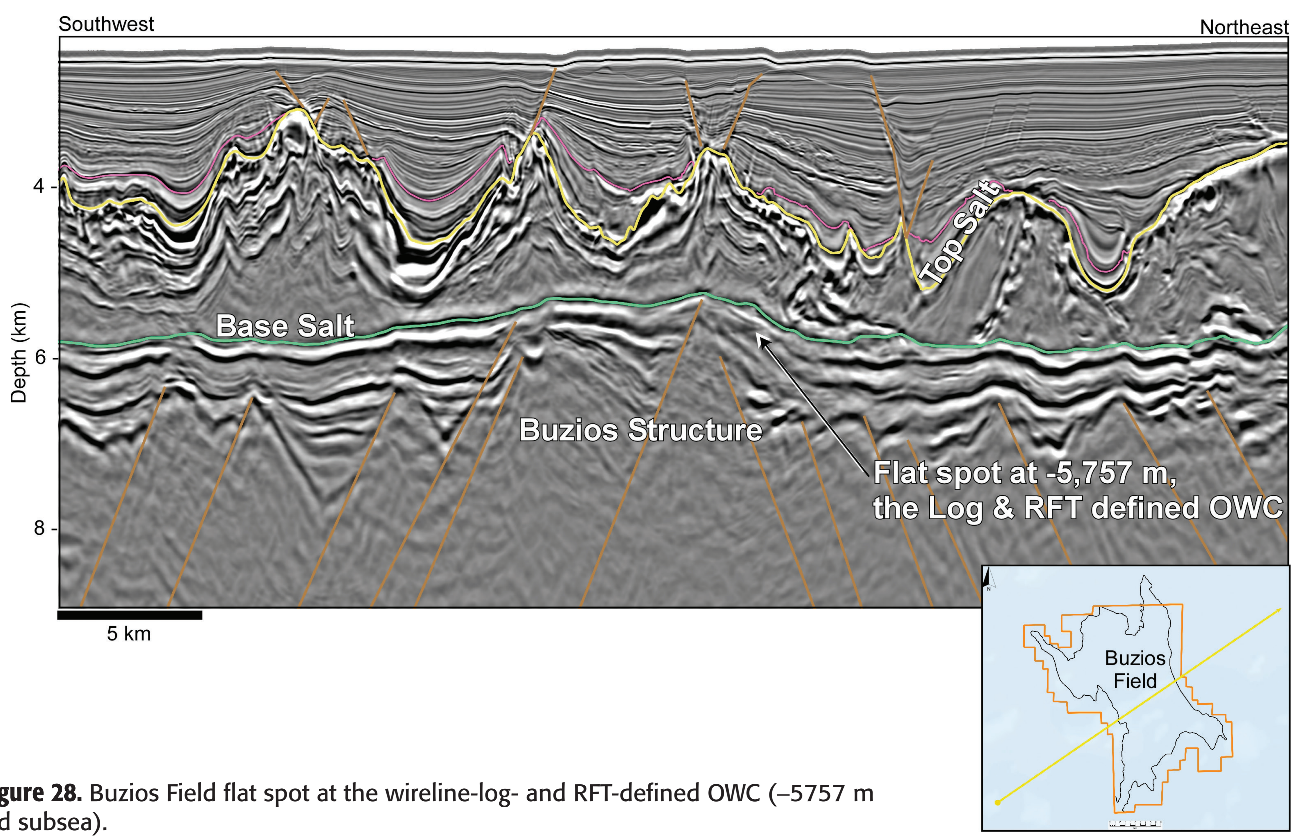

Figure 28. Buzios Field flat spot at the wireline-log- and RFT-defined OWC (–5757 m tvd subsea).

hydrocarbons migrate upsection to overlying Albian, Cretaceous, and Tertiary reservoirs. Basinward, the play fairway is controlled by the distribution of synrift source rocks, which is controlled by the position of the COB. Although the distribution of pre-salt microbialite reservoirs is somewhat restricted, underlying coquina reservoirs are widespread. They are present on the shelf and in deep water, from the southern Santos Basin northward to the Campos Basin Jubarte Field, and possibly beyond.

Within the defined play fairway, pre-salt accumulations occur in four-way-dip structural closures, fault-bounded three-way-dip structural closures, and three-way-dip structural closures onlapping synrift or basement structural highs. Nearly all hydrocarbon accumulations are associated with base salt structural highs that are coincident with pre-salt isopach thins (Figure 25).

IMPLICATIONS FOR FIELD DEVELOPMENT

In addition to its role in pre-salt exploration, the Picanha 3-D seismic data volume has important development applications, at both field and reservoir scales. Buzios Field, a multibillion barrel recoverable pre-salt field on the Santos Basin Outer High (Figures 1, 2, 8, 14, 16, 25), is used as an example. As of March 2020, Buzios Field Barra Velha reservoirs were producing 640,000 BOPD (790,000 BOEPD total) from four platforms (Offshore, 2020).

Integrated Pre-Salt Reservoir Characterization Workflow

An integrated reservoir characterization workflow was developed for quantitative interpretation

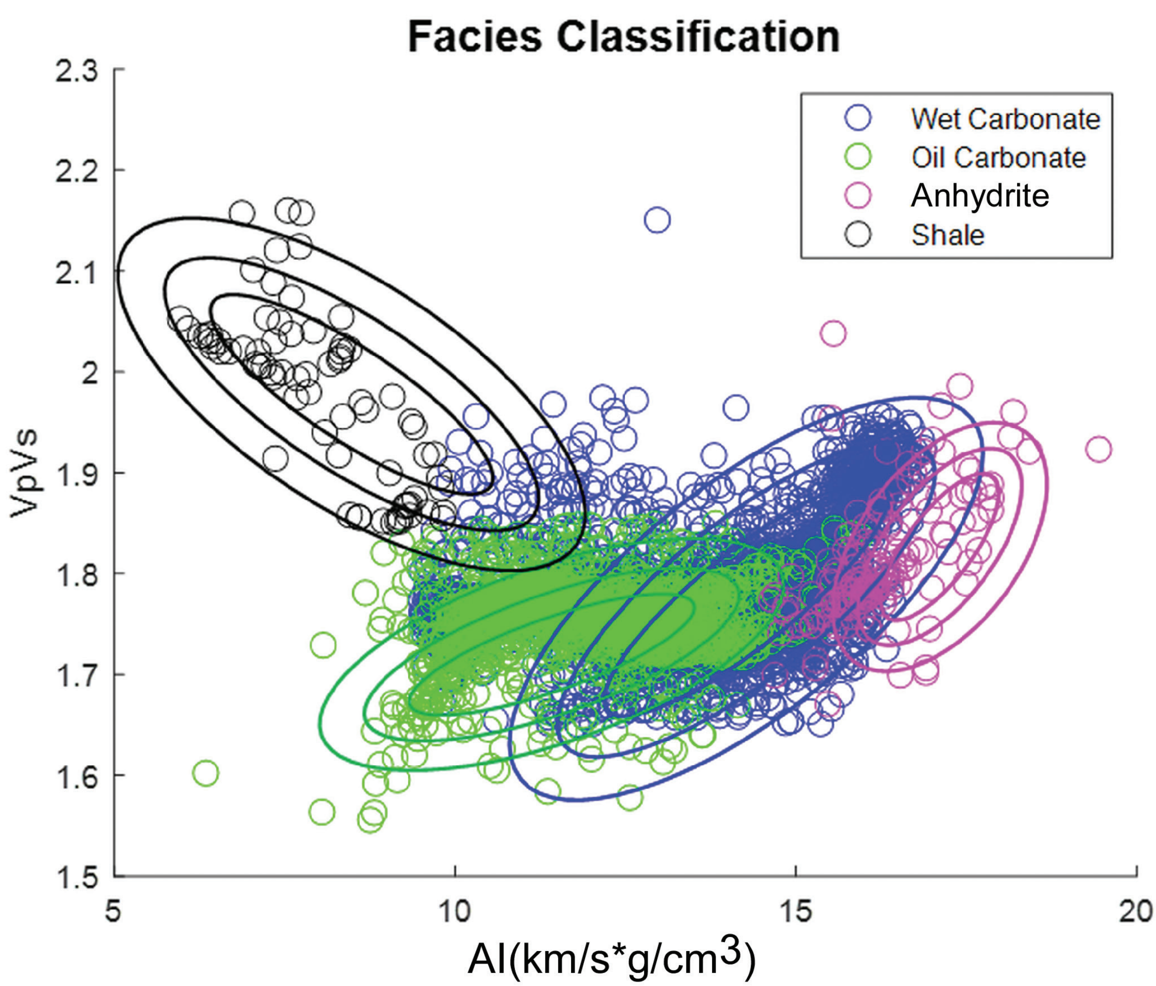

Figure 29. Rock physics diagnostics and lithofacies classification. Multi-well cross-plot of AI vs. Vp/Vs ratio, color-coded by facies. Probability density functions, estimated from cluster analysis, are also plotted.

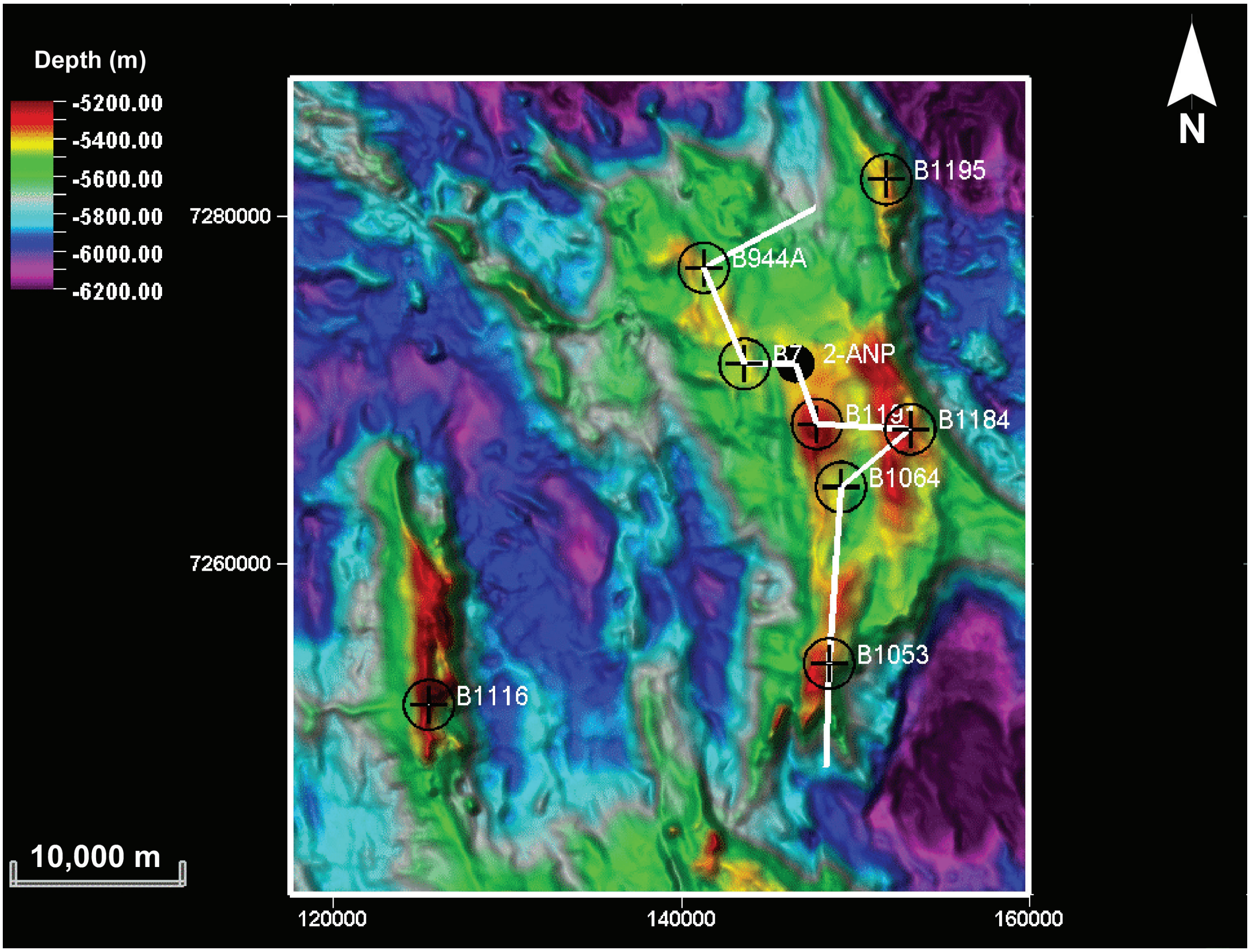

Figure 30. A top reservoir (base-salt) 3-D depth structural image of Buzios Field showing the location of the arbitrary line.

of Buzios Field pre-salt reservoirs. The workflow includes petrophysical analysis, rock physics diagnostics, lithofacies classification, AVO inversion, reservoir property prediction, and data analytics (Figure 26).

Data analytics, more widely referred to as "machine learning," serves as an alternative tool for improved seismic interpretation and reservoir characterization where data quality is poor, petrophysical relationships are ambiguous, and data are limited. Data analytics, including multivariate regression, Bayesian classification/regression, and neural network algorithms, are widely used in log data prediction, facies classification, and reservoir properties prediction when incorporated with AVO inversion products (Hampson et al., 2001; Zhou et al., 2013; Alvarez et al., 2015). At Buzios Field, data analytic tools that use an attribute selection scheme, namely, step-wise regression, are used to improve the traditional reservoir characterization practice.

Data from eight Buzios wells and the Picanha 3-D seismic data volume form the reservoir characterization data set. Of these eight wells, seven have mud logs and the log suite required for conventional well analysis. The discovery well 2-ANP-1-RJS (Figure 27) is used to demonstrate Buzios Field reservoir lithology, porosity, and fluid types.

Reservoir Characterization Results

Limestone is the dominant reservoir lithology at Buzios Field (Figure 27). Resistivity data from multiple Buzios wells define a generally consistent, sharp oil–water contact (OWC) at −5757 m TVD subsea. This resistivity-defined contact is consistent with the Repeat Formation Tester (RFT)-defined OWC at the 3-BRSA-1184-RJS well. Both occur at a depth

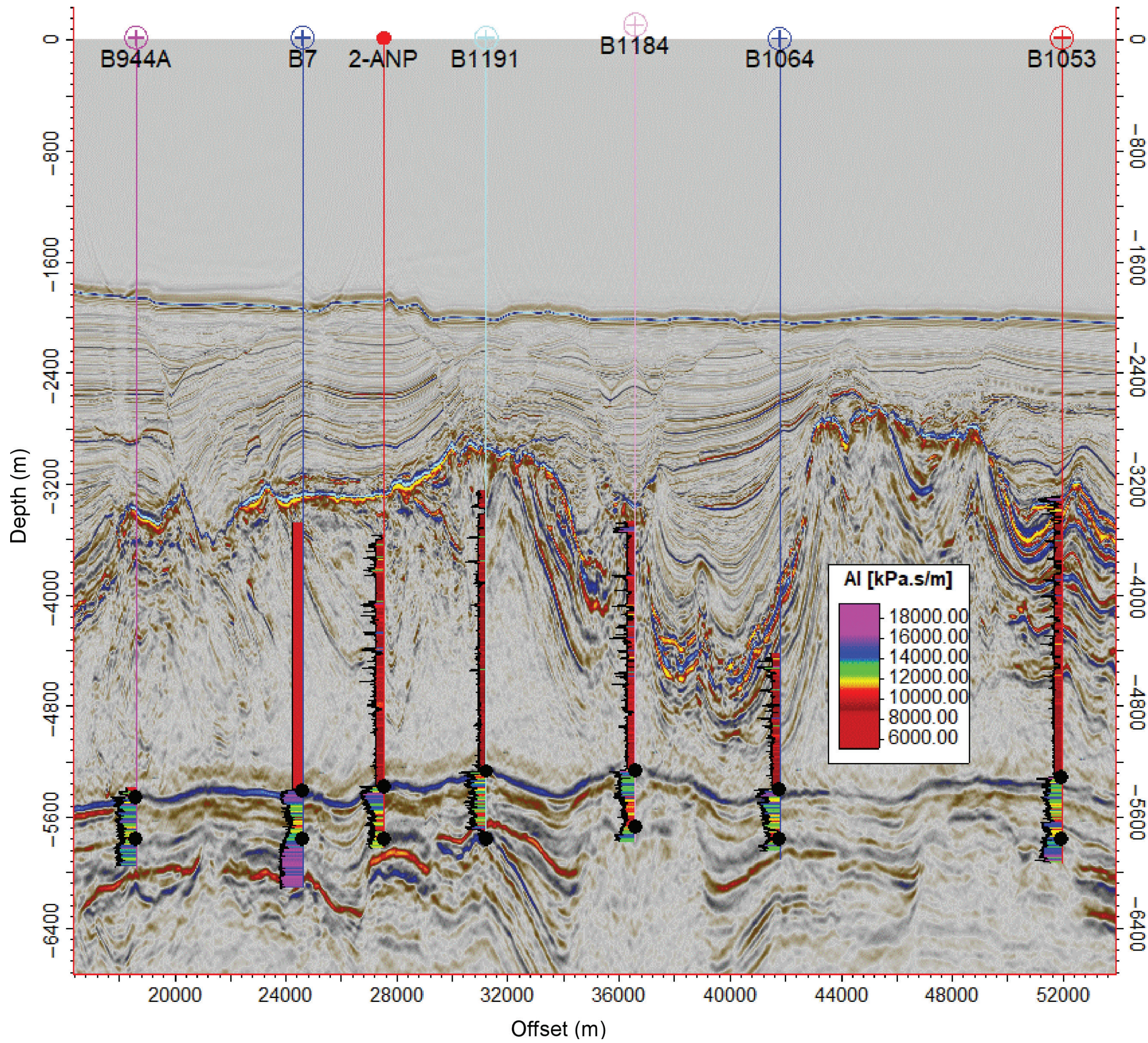

Figure 31. Arbitrary Acoustic Impedance seismic profile through Buzios Field. P-impedance logs are shown at well locations. Upper black dots indicate the base-salt horizon; lower black dots indicate the oil-water contact.

consistent with a clearly defined flat spot on full-stack PSTM seismic data (Petersohn et al., 2013; Figure 28).

In the 2-ANP-1-RJS well, reservoir porosity ranges from 10% to 20%. Oil saturation ranges from 75% to 85% above the OWC. Four lithofacies are defined from interpreted lithology and fluid type: wet carbonate (Sw >70%), oil-saturated carbonate (So >70%), shale (shale volume >60%), and anhydrite (anhydrite >60%; Pedrosa Jr. et al., 2021).

Rock Physics Diagnostics and Facies Classification

Using Buzios field Vp/Vs and acoustic impedance (AI) data, we investigate the elastic response of each pre-salt lithofacies (Figure 29). Shale-rich intervals have the highest Vp/Vs ratio (>1.85). High oil saturation occurs predominantly in porous carbonates, with an elastic signature comprising low AI and low Vp/Vs ratios. In contrast, water-saturated, low-porosity carbonates have an elastic signature comprising high AI and Vp/Vs ratios lower than 1.9. Oil- and water-saturated lithofacies overlap in this cross-plot, thus the fluid response is not diagnostic in the AI, approximately Vp/Vs domain. Despite this, they can be differentiated using the detailed classification workflow described next.

To further test the elastic response sensitivity of each facies, the statistical rock physics (SRP) classification (Zhou et al., 2013) is employed. The SRP workflow uses the Naive Bayesian classification scheme to estimate the probabilities of each facies, given the clustered distribution in the selected elastic domain. The predicted facies are assigned with the maximum probability.

AVO Inversion

A low-frequency background velocity model for pre-stack seismic inversion is constructed by interpolating and extrapolating well-log measurements with guidance from the interpreted base salt surface. The AVO inversion is performed with a pre-stack simultaneous inversion algorithm.

P-impedance and Vp/Vs ratio inversion results for an arbitrary north–south transect through Buzios Field (Figure 30) are shown in Figures 31 and 32. A basal shale is clearly identified from a relatively high Vp/Vs ratio. Overlying Barra Velha reservoirs show a relatively homogeneous Vp/Vs ratio varying in the range of 1.70 to approximately 1.75. In contrast, among the carbonate layers, the AI shows a relatively large variation with porous carbonate characterized by relatively low AI.

Reservoir Properties Prediction

Data analytics techniques are used to delineate the reservoir porosity and fluid saturation for resource estimation and reservoir management. Various multivariate regression and neural network predictions are used, methods that may provide results superior to conventional quantitative reservoir characterization.

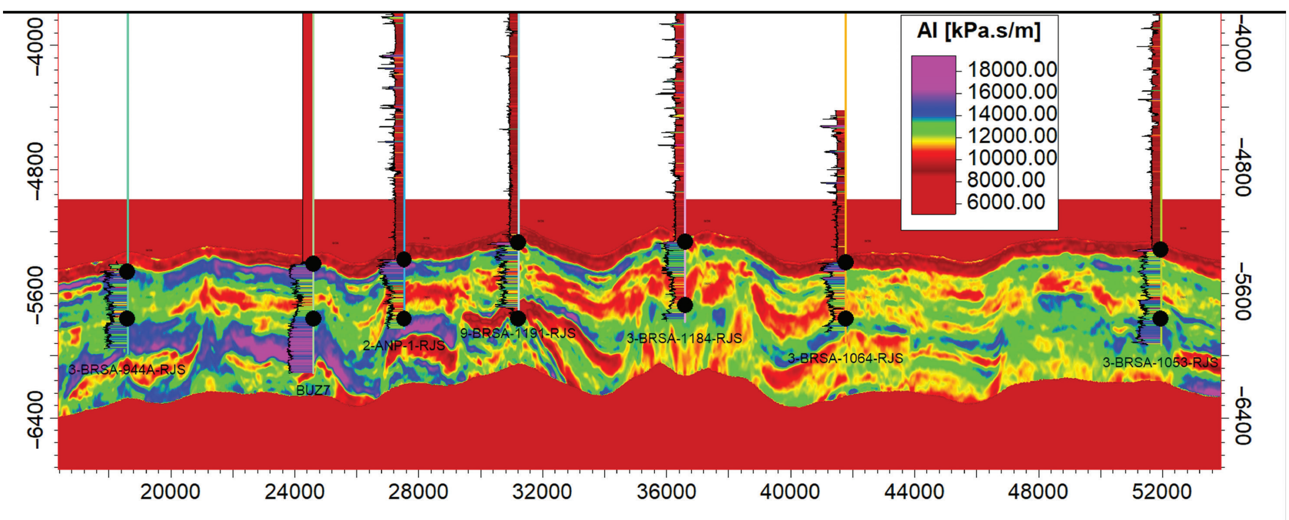

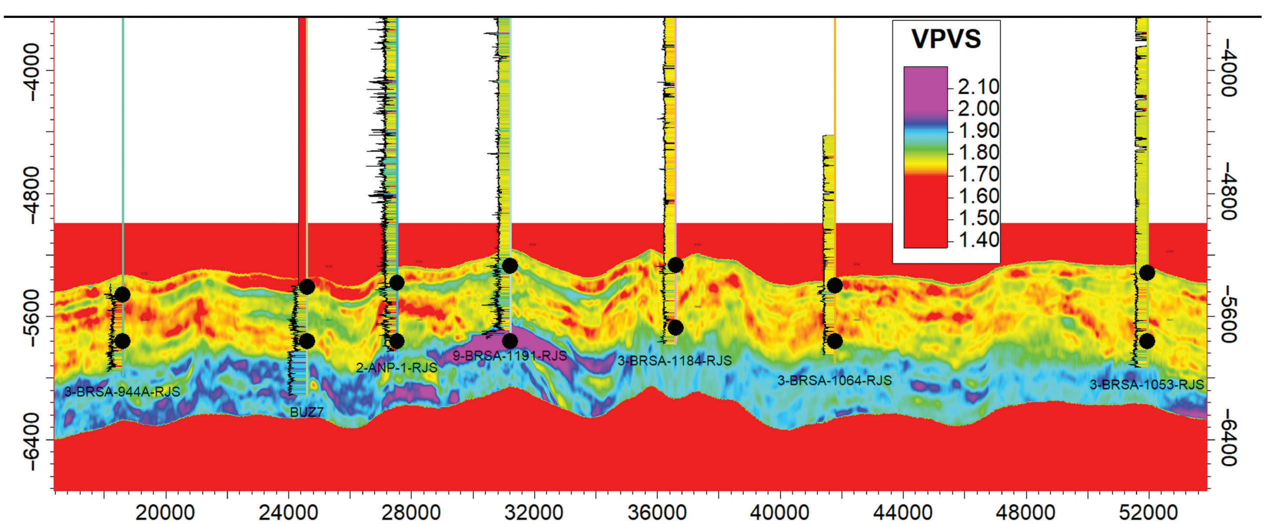

Figure 32. Inversion results on the Buzios Field arbitrary line. Acoustic Impedance (top); Vp/Vs ratio (bottom). Corresponding well logs are overlain on the sections to validate inversion results.

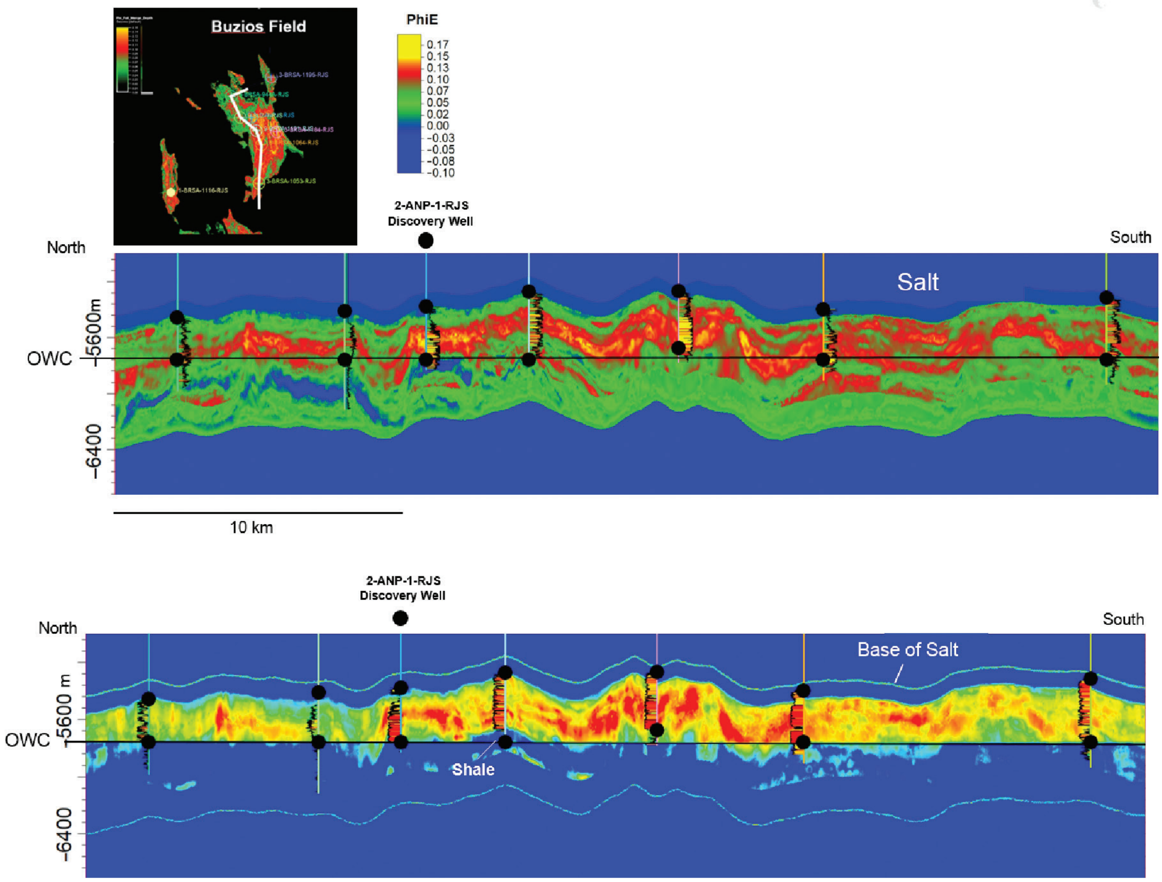

Figure 33. Predicted effective porosity (top) and water saturation (bottom) along the arbitrary line shown in Figure 30. Well-log interpreted results are overlain on the predicted section seismic data.

The porosity prediction uses inverted impedance, Vp/Vs, and facies, together with attributes from the seismic data itself. The predicted porosity is added to the attribute pool for water saturation prediction.

Figure 33 shows the predicted effective porosity (top) and water saturation (bottom), on the arbitrary line referred to above. Predicted results are consistent with conventional petrophysical interpretation using a full suite of logs at all wells. Oil-saturated rocks are concentrated principally in areas with low impedance and high porosity. The independent petrophysical log and RFT data are integrated with the predicted saturation volume to ensure the consistency of multiple physics measurements. Results suggest good reservoir quality in the center of the field, degrading to the north and the south. They also reveal the field's structural complexity and demonstrate that reservoir porosity is quite heterogeneous (Figure 34).

Well log data and seismic inverted elastic attributes indicate that reimaged regional seismic data are effective for the quantitative characterization of pre-salt Barra Vella reservoirs. Vp/Vs ratios discriminates carbonate rocks from shales, hence is a reliable lithology indicator. Similarly, the P-impedance aids in the prediction of reservoir quality in carbonate facies as well as serving as a porosity/fluid indicator. The high quality of the seismic data and the robust reservoir characterization workflow ensure that predicted reservoir properties are consistent with well logs, hence are geologically sound.

CONCLUSIONS

The Picanha 3-D megaregional data volume, in combination with data from 174 wells and regional 2-D data, has enabled definition of the Santos Basin pre-salt play fairway.

- The play extends from the southern Santos Basin to the Campos and Espirito Santo basins, over an area of approximately 210,000 km^2. The presence

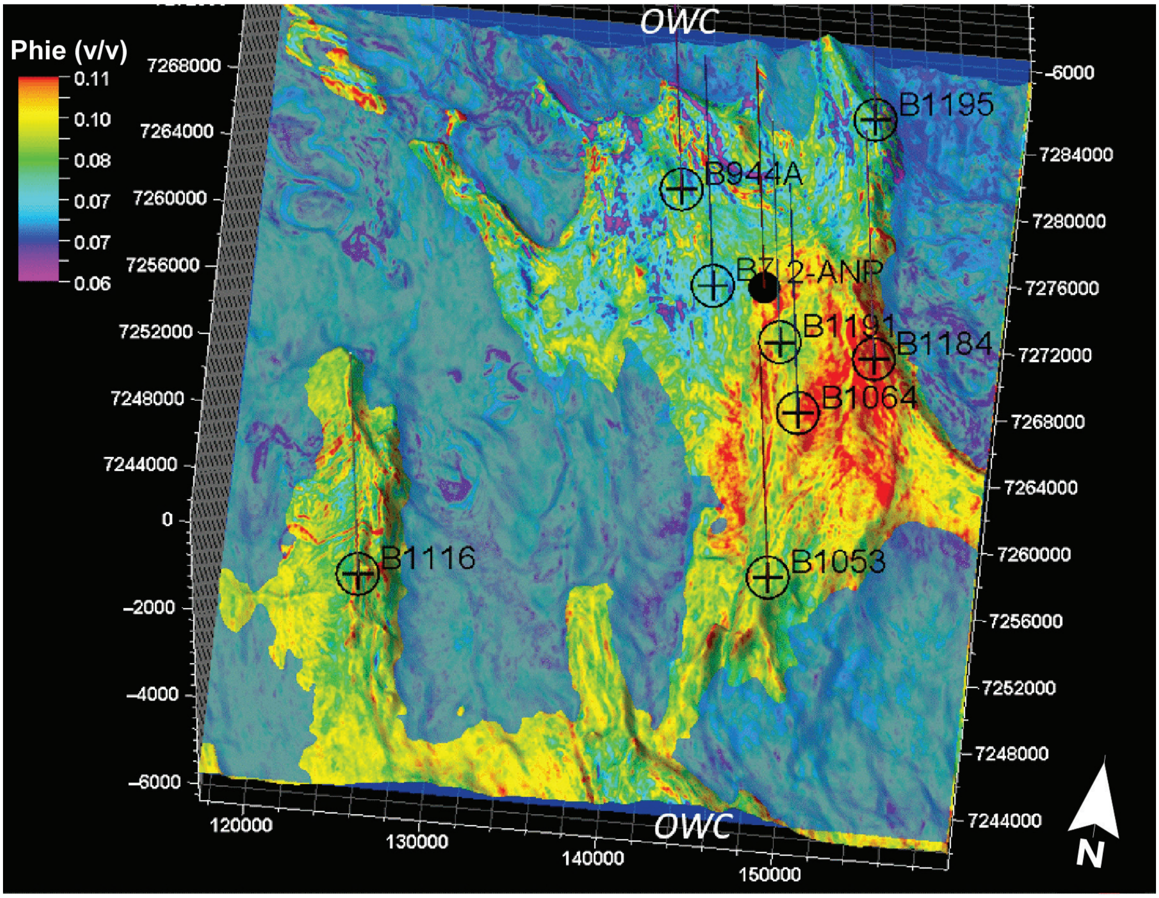

Figure 34. Average porosity above Buzios Field's OWC (blue slice), co-rendered with top reservoir (base-salt) 3-D depth structure. Note reservoir heterogeneity and the increase in porosity over the crest of the structure.

of many undrilled traps within the pre-salt play fairway, coupled with creaming curve analysis, suggests the pre-salt play has billions of barrels of remaining resource potential.

- The inboard (western) extent of the pre-salt play fairway is controlled by the limit of the Aptian salt seal. In areas where salt is absent, pre-salt hydrocarbons migrate upsection to overlying Albian, Cretaceous, and Tertiary reservoirs.
- Basinward, the play fairway is controlled by the distribution of synrift source rocks, which is controlled by the position of the COB.
- Although the distribution of pre-salt microbialite reservoirs is somewhat restricted, underlying coquina reservoirs are widespread. They are present on the shelf and in deep water, from the southern Santos Basin Caramba Field to the deep-water Campos Basin Jubarte Field and possibly beyond.
- Within the play fairway area, pre-salt accumulations occur in four-way-dip structural closures, fault-bounded three-way-dip structural closures, and three-way-dip structural closures onlapping synrift or basement structural highs. Nearly all hydrocarbon accumulations are associated with base salt structural highs that are coincident with pre-salt isopach thins. Within these areas, reservoir quality improves over the crest of the structures and diminishes downdip.

The Santos Basin Outer High hosts the largest oil and gas fields discovered in Brazil to date.

- The Santos Basin Outer High is an area of regional migration focus, fetching thermally mature, oil-prone kitchen areas to the west, north, and east.
- During mid-to-late Aptian time, it was a clastic-starved area, favorable for development of thick (>600 m) pre-salt lacustrine carbonate reservoirs.
- It is an area containing a greater than 2000 m thick salt seal and multiple large pre-salt structural closures.

- In this area, oil columns locally exceed 600 m in height.
- The area contains an extraordinary combination of high-storage-capacity, high-deliverability, undersaturated, and overpressured lacustrine carbonate reservoirs and excellent crude oil quality in areas that are not CO_2 rich.

At field and reservoir level, inverted elastic seismic attributes and data analytics are effective for quantitative characterization of the pre-salt reservoirs. Vp/Vs ratios discriminate carbonate lithologies from shales, hence are a reliable reservoir indicator. Similarly, AI aids in the prediction of carbonate reservoir quality and serves as a porosity/fluid indicator.

ACKNOWLEDGMENTS

The authors thank ION Geophysical for its support and gracious permission to publish proprietary seismic data. The authors also thank the members of ION's processing and interpretation groups for their arduous merging and reimaging of an immense volume of 3-D seismic data. We thank Mr. Yijie Zhou for his significant contributions to Buzios Field reservoir characterization.

We thank Dr. Marcio Mello for the opportunity to contribute to this volume, and we are grateful to Mr. Nick Maden and Mr. Mark Shann for their constructive reviews of the manuscript.

REFERENCES CITED

Alvarez, P., F. Bolívar, M. Di Luca, and T. Salinas, 2015, Multiattribute rotation scheme: A tool for reservoir property prediction from seismic inversion attributes: Interpretation, v. 3, no. 4, p. SAE9–SAE18.

ANP Bulletin, 2020, Boletim da Produção de Petroleo e Gas Natural, 111, 36 p., accessed August 10, 2020, http://www.anp.gov.br/arquivos/publicacoes/boletins-anp/producao/2019-11-boletim.pdf.

Ávila, R., M. Abelha, and E. Petersohn, 2017, Peroba, Pau Brasil e Alto de Cabo Frio, Agencia Nacional de Petroleo (ANP), Pré-Sal Brasil, Partilha de Produção: Seminários Técnicos, 44 p.

Boyd, A., A. Souza, G. Carneiro, V. Machado, W. Trevizan, B. Santos, P. Netto, R. Bagueira, R. Polinski, and A. Bertolini, 2015, Presalt carbonate evaluation for Santos Basin, offshore Brazil: Petrophysics, v. 56, no. 6, p. 577–591.

Cardoso, R. A. and V. M. Hamza, 2014, Heat flow in the Campos Sedimentary Basin and thermal history of the continental margin of southeast Brazil: International Scholarly Research Notices, accessed February 9, 2021, https://www.hindawi.com/journals/isrn/2014/384752/.

Ceraldi, T. S. and D. Green, 2016, Evolution of the South Atlantic lacustrine deposits in response to Early Cretaceous rifting, subsidence and lake hydrology: Petroleum Geoscience of the West Africa Margin: Geological Society of London Special Publication, v. 438, no. 1, p. 77–98.

Corbett, P. W. M., 2015, Reservoir Characterisation Challenges in Pre-Salt Brazilian Carbonates: Search and Discovery Article #51083 (2015), adapted from oral presentation given at AAPG Geoscience Technology Workshop, Carbonate Plays around the World—Analogs to Support Exploration and Development, New Orleans, Louisiana, February 4–5, accessed February 9, 2021, http://www.searchanddiscovery.com/pdfz/documents/2015/51083corbett/ndx_corbett.pdf.html.

Dahl, J. E., J. M. Moldowan, and M. R. Mello, 2021, Diamondoid nanotechnology reveals migration pathways and mixing in Santos Basin pre-salt oils, *in* Marcio R. Mello, Pinar O. Yilmaz, and Barry J. Katz, eds., The supergiant Lower Cretaceous pre-salt petroleum systems of the Santos Basin, Brazil: AAPG Memoir 124, p. 107–118.

Elias, A., S. Mello, D. Schiozer, and V. Trevisan, 2014, PVT analysis process of pre-salt similar oil associated with compositional simulation, Rio Oil & Gas Conference, pp. IBP2051_14.

Formigli, J., A. Pinto, and A. Almeida, 2009, Santos Basin's pre-salt reservoirs development—the way ahead, Paper OTC-19953 presented at the Offshore Technology Conference, Houston, Texas, USA, May 4–7, DOI: 10.4043/19953-MS.

Fruehn, J., S. Greenwood, R. O'Driscoll, I. Jones, and J. Brittan, 2019, A strategy for regional-scale FWI in the salt provinces offshore Brazil: 16th International Congress of the Brazilian Geophysical Society, Rio de Janeiro, Brazil, August 17–23, accessed February 9, 2021, https://library.seg.org/doi/abs/10.1190/segam2019-3201719.1.

Gomes, P. O., B. Kilsdonk, J. Minken, T. Grow, and R. Barragan, 2009, The outer high of the Santos Basin, southern São Paulo Plateau, Brazil: Pre-salt exploration outbreak, paleogeographic setting, and evolution of the syn-rift structures: Search and Discovery Article #10193, accessed December 17, 2020, http://www.searchanddiscovery.com/documents/2009/10193gomes/index.htm.

Hampson, D. P., J. S. Schuelke, and J. A. Quirein, 2001, Use of multiattribute transforms to predict log properties from seismic data: Geophysics, 66, no. 1, p. 220–236.

Hurst, N., E. Kay, and A. Cannell, 2020, NamibeSPAN Interpretation Report, proprietary ION Geophysical Report, 46 p.

IHS Markit, 2020, E&P Data Worldwide (proprietary digital database), Houston, Texas, U.S.A., accessed February 9, 2021, https://ihsmarkit.com/index.html.

Kemna, H. A., M. R. Mello, W. Peres, S. P. Rostirolla, and D. Palmowski, 2021, Workflows and interpretation of regional 3-D petroleum systems modeling: An example from the deep-water pre-salt realm of the Santos Basin, Brazil, *in* Marcio R. Mello, Pinar O. Yilmaz, and Barry J Katz, eds., The supergiant Lower Cretaceous pre-salt petroleum systems of the Santos Basin, Brazil: AAPG Memoir 124, p. 325–350.

Mello, R. M., C. Bisel, H. Kemna, J. Dahl, J. M. Moldowan, and S. P. Rostirolla, 2020, The hydrocarbon exploration potential of the outboard region of the Santos Basin application of integrated multiparameter studies as a game changer in reducing the oil and gas exploration risk assessment, FM-3808-00: Rio oil and Gas Expo and Conference 2020, 10 p.

Mello, M. R., S. P. Rostirolla, V. Elias, M. Ferreira, A. P. Ahualli, S. Becker, J. E. Dahl, and J. M. Moldowan, 2021, Lacustrine source rocks and oil systems present in the Lower Cretaceous pre-salt section of the Santos Basin, Brazil, *in* Marcio R. Mello, Pinar O. Yilmaz, and Barry J Katz, eds., The supergiant Lower Cretaceous pre-salt petroleum systems of the Santos Basin, Brazil: AAPG Memoir 124, p. 33–74.

Moreira, J. L. P., C. V. Madeira, J. A. Gil, and M. A. Pinheiro Machado, 2007, Bacia de Santos: Boletim de Geociências da Petrobras, v. 15, p. 531–549.

Offshore, 2020, Búzios offshore Brazil producing at record volumes, Petrobras claims: Offshore, accessed February 9, 2021, https://www.offshore-mag.com/production/article/14169769/deepwater-bzios-oil-and-gas-field-offshore-brazil-producing-at-record-volumes-petrobras-claims.

Offshore Technology, 2018, Buzios Field, Santos Basin: Offshore-technology.com, accessed July 2020, https://www.offshore-technology.com/projects/buzios-formerly-franco-field-cesso-onerosa-region-santos-Basin/.

Pedrosa Jr., O. A., W. Peres, M. R. Mello, S. P. Rostirolla, G. Carmo Jr., and V. Branco, 2021, Challenges for reservoir management and field development in the pre-salt, Santos Basin, Brazil, *in* Marcio R. Mello, Pinar O. Yilmaz, and Barry J Katz, eds., The supergiant Lower Cretaceous pre-salt petroleum systems of the Santos Basin, Brazil: AAPG Memoir 124, p. 175–192.

Petersohn, E., M. Abelha, and L. Pedrosa, 2013, Brazil pre-salt Libra Geological Assessment and Environmental Overview: ANP (National Agency of Petroleum, Natural Gas and Biofuels) presentation, accessed September, 2020, http://rodadas.anp.gov.br/arquivos/Round_P1/Seminarios_P1/Apresentacoes/partilha1_tecnico_ambiental_ingles.pdf

Pindell, J., R. Graham, P. Bellingham, K. McDermott, M. Kaminski, B. Horn, and D. Paton, 2015, Continental margin formation and creation of "Lateral Tectonic Accommodation Space" for salt deposition, Campos and Santos basins, São Paulo Plateau, Brazil, *in* Paul J. Post, James Coleman Jr., Norman C. Rosen, David E. Brown, Tina Roberts-Ashby, Peter Kahn, Mark Rowan, eds., Petroleum Systems in "Rift" Basins, Petroleum Systems in "Rift" Basins 34th Annual Gulf Coast Section SEPM Foundation Perkins-Rosen Research Conference, p. 787–788, DOI: 10.5724/gcs.15.34.0787.

Sandwell, D. T., R. D. Müller, W. H. F. Smith, E. Garcia, and R. Francis, 2014, New global marine gravity model from Cryo-Sat-2 and Jason-1 reveals buried tectonic structure: Science, v. 346, no. 6205, p. 65–67, DOI: 10.1126/science.1258213.

Schroder, S., A. Ibekwe, M. Saunders, R. Dixon, and A. Fisher, 2016, Alga-microbial carbonates of the Namibe Basin (Albian, Angola): Implications for microbial carbonate mound development in the South Atlantic: Petroleum Geoscience, v. 22, p 71–90.

Thompson, D. L., J. D. Stilwell, and M. Hall, 2015, Lacustrine carbonate reservoirs from Early Cretaceous rift lakes of Western Gondwana: Pre-salt coquinas of Brazil and West Africa: Gondwana Research, v. 28, no. 1, p. 26–51.

Zhou, Y., Z. Hossain, and M. Ellis, August 2013, Advancing Statistical Rock Physics Capabilities for Lithofacies Prediction: Second International Workshop on Rock Physics, Southampton, United Kingdom, accessed February 9, 2021, https://www.earthdoc.org/content/papers/10.3997/2214-4609-pdb.381.Zhou_et_al.